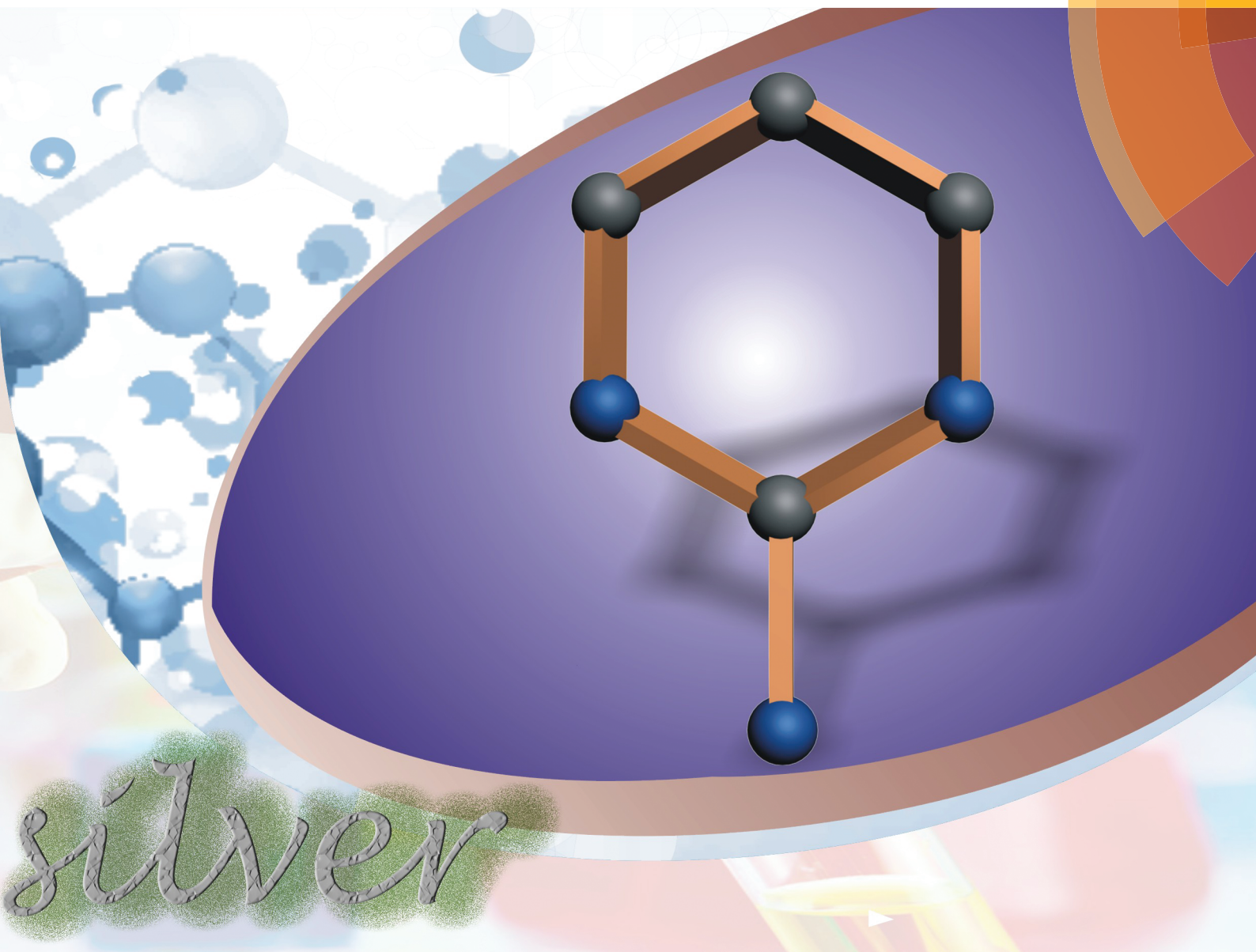


# CrystEngComm

[www.rsc.org/crystengcomm](http://www.rsc.org/crystengcomm)



ROYAL SOCIETY  
OF CHEMISTRY

HIGHLIGHT

Di Sun *et al.*

Luminescent silver(i) coordination architectures containing 2-aminopyrimidyl ligands



Cite this: *CrystEngComm*, 2015, 17,  
3393

## Luminescent silver(I) coordination architectures containing 2-aminopyrimidyl ligands<sup>†</sup>

Xing-Po Wang,<sup>‡,a</sup> Tuo-Ping Hu,<sup>‡,b</sup> and Di Sun<sup>a\*</sup>

The design and assembly of new coordination architectures is nowadays a challenging research field that attracts increasing attention due to the unique structural and functional properties of such metal-organic materials. The selection of suitable organic ligands as building blocks is one of the most important points for the construction of novel coordination architectures with fascinating structures and functions. In contrast to the recognized use of some N heterocyclic ligands for the construction of coordination architectures, 2-aminopyrimidine ( $\text{NH}_2\text{pym}$ ) and its related derivatives are simple, commercially available, soluble and highly versatile angular building blocks, but still underdeveloped until now. Given the high potential of this kind of ligands for future developments in this research field, the present highlight will review the coordination-driven assembly of 2-aminopyrimidyl building blocks with or without auxiliary ligands with closed-shell  $d^{10}$   $\text{Ag}(\text{I})$  ions as well as their luminescence properties. Multiplicity of the established structural motifs thus far (only considering the coordination interaction) is outlined, illustrating the broad range of coordination motifs from 0D discrete molecular architectures to infinite extended one-, two-, and three-dimensional (1-D, 2-D, and 3-D) networks. The specific influencing factors such as anion, auxiliary ligand, substituent, and solvent on structural assemblies and the fluorescence of these crystalline solids are also discussed.

Received 2nd February 2015,  
Accepted 2nd March 2015

DOI: 10.1039/c5ce00238a

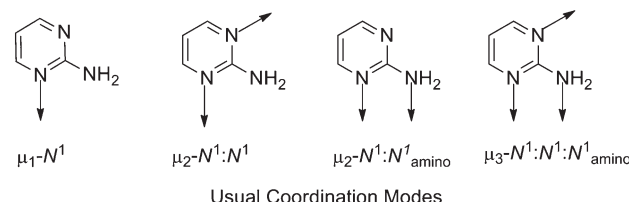
[www.rsc.org/crystengcomm](http://www.rsc.org/crystengcomm)

## 1. Introduction

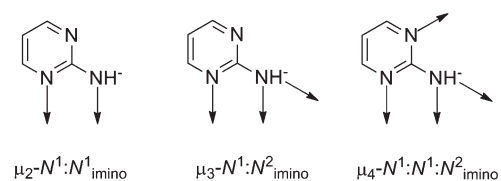
The crystal engineering of new coordination architectures is currently one of the far-reaching research fields in coordination, supramolecular and materials chemistry, which also attracts momentous attention due to the diverse structural motifs and potential applications.<sup>1</sup> Among the variety of organic ligands, different N heterocyclic ligands such as poly-pyridyl and polyimidazolyl ligands have been broadly explored as linkers for the construction of coordination networks.<sup>2</sup> Much research has also been focused on the design and synthesis of new organic molecules with tunable properties toward their use in crystal engineering.<sup>3</sup> Surprisingly, the potential of some simple organic heterocyclic ligands that possess all the requirements to become common building blocks for the assembly of coordination architectures has not been fully realized.

2-Aminopyrimidine ( $\text{NH}_2\text{pym}$ ) can be considered as one such simple heterocyclic compound, which, due to its

inexpensiveness, commercial availability, high solubility in water and polar organic solvents, has found a broad variety of applications such as antifolate drugs in medicinal chemistry and precursors in organic synthesis.<sup>4</sup> With regard to coordination chemistry,  $\text{NH}_2\text{pym}$  and its derivatives are versatile ligands because of documented metal binding patterns (Scheme 1) including the ring nitrogen atom<sup>5</sup> or the exocyclic amino group,<sup>6</sup> occasionally in equilibrium, and simultaneously both positions, either in a chelating or bridging



Usual Coordination Modes



Unusual Coordination Modes

**Scheme 1** Coordination modes of  $\text{NH}_2\text{pym}$  found in silver coordination compounds.

<sup>a</sup> Key Lab of Colloid and Interface Chemistry, Ministry of Education, School of Chemistry and Chemical Engineering, Shandong University, Jinan, 250100, PR China. E-mail: dsun@sdu.edu.cn; Fax: +86 531 88364218

<sup>b</sup> Department of Chemistry, North University of China, Taiyuan, Shanxi 030051, People's Republic of China

† Electronic supplementary information (ESI) available. See DOI: 10.1039/c5ce00238a

‡ These authors contributed equally.

fashion.<sup>7</sup> Moreover, the stereochemically associative amino group also demonstrated ability to form very stable hydrogen-bonded arrays.<sup>8</sup> Recent studies also revealed its rare coordination modes realized by the deprotonation of the amino group through a N–H activation process.<sup>9</sup> In addition, as a good H-bond donor and acceptor, supramolecular architectures through self assembly by hydrogen bonding or by co-crystallization especially with themselves or carboxylic acids for enhanced hydrogen bonding motifs were widely observed, *e.g.* capsules with resorcin[4]arenes.<sup>10</sup> Such a simple molecule with rich coordination modes endows it as a versatile ligand to construct the rich families of coordination architectures.

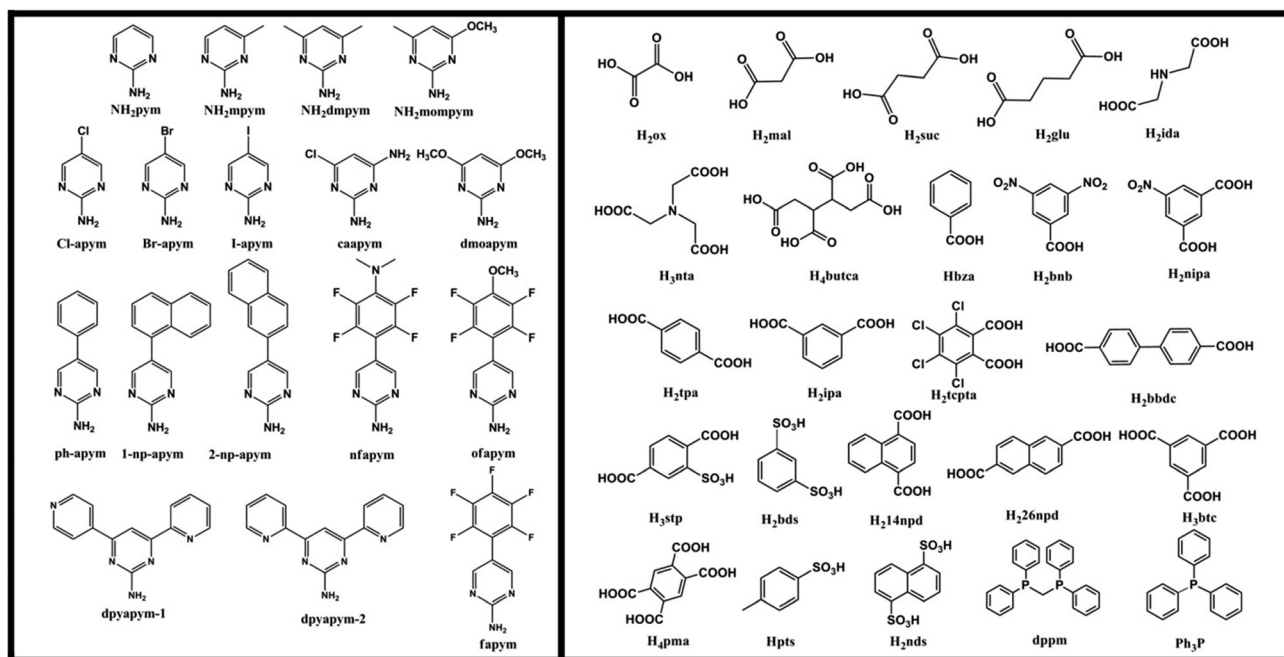
The first coordination compound of NH<sub>2</sub>pym dates back to 1969 when Weiss *et al.* noticed that NH<sub>2</sub>pym and transition metal ions can form coordination compounds.<sup>11</sup> As there are many references on coordination compounds of NH<sub>2</sub>pym and its derivatives, for obvious reasons, we only focus on silver-based coordination compounds herein. A review of the coordination polymers of Ag(I) and heterocyclic N-donor ligands has been published by Schröder's group in 2001.<sup>12</sup> Compared to other common N-donor ligands such as 4,4'-bipyridine, 2,2'-bipyridine and pyrazine thousands of hits have been found in the Cambridge Structural Database (CSD),<sup>13</sup> the use of NH<sub>2</sub>pym and its derivatives as a simple and convenient linker with an angular geometry for the assembly of coordination architectures with transition metals, especially Ag(I), was explored to a lesser extent.

Given the fact that this area of research on coordination architectures of NH<sub>2</sub>pym and its derivatives has not yet been reviewed in spite of the upsurge of new structures and great potential for future developments, the present work consists

of (i) an overview of the structural and topological types of silver(I)-NH<sub>2</sub>pym and its derivative coordination architectures with or without auxiliary ligands (Scheme 2), (ii) a discussion of some novel coordination architectures involving unusual deprotonation of amino in NH<sub>2</sub>pym and its derivatives, (iii) the summary of influence factors on assembly in this system and (iv) the summary of luminescence properties of selected coordination architectures in this family.

## 2. General considerations

Within the structurally characterized compounds based on NH<sub>2</sub>pym and its derivatives reported to date, 110 silver coordination compounds have been identified by searching the CSD, wherein NH<sub>2</sub>pym and its derivatives possess at least one coordination bond to an Ag(I) center. They are divided into four sub-groups, 0D (1–25), 1D (26–74), 2D (75–100) and 3D (101–110) networks, which are summarized in Tables 1–4, respectively. Among them, a few but important examples bear rare deprotonated NH<sub>2</sub>pym or NH<sub>2</sub>dmpym as a bridging ligand and represent a tiny but interesting group of NH<sub>2</sub>pym and its derivative supported coordination compounds. The distribution of coordination modes of NH<sub>2</sub>pym in all compounds is shown in Scheme 3. The first Ag(I) coordination compound of NH<sub>2</sub>pym dates back to 1998 when Smith *et al.* reported two structure motifs of NH<sub>2</sub>pym and NH<sub>2</sub>dmpym with Ag(I) and *p*-toluenesulfonate,<sup>14</sup> following this work, only sporadic examples of this series were reported until 2005. From 2006 to 2014, the flourishing progress of crystal engineering yielded more than 100 new structures in this system, more than half of them were reported within the last three years. Bearing these features in mind and expecting even



Scheme 2 Structures of NH<sub>2</sub>pym and its derivatives, auxiliary ligands and corresponding abbreviations for them in this highlight.

**Table 1** A summary of the 0D structures in this highlight

Complex	Refcode	Space group	Formula	Nuclearity	Coordination number of Ag	Coordination mode of ligand	Ref.
1	BUDDUA	<i>Pbc2</i> <sub>1</sub>	[Ag(NH <sub>2</sub> pym) <sub>2</sub> ]·NO <sub>3</sub>	1	2	μ <sub>1</sub> -N <sup>1</sup>	20
2	BURQUB	<i>Pccn</i>	[Ag <sub>2</sub> (NH <sub>2</sub> pym) <sub>3</sub> (bnb)]·0.34H <sub>2</sub> O	2	3	μ <sub>1</sub> -N <sup>1</sup> and μ <sub>2</sub> -N <sup>1</sup> :N <sup>1</sup>	21
3	EXAXAD	<i>C2/c</i>	[Ag <sub>2</sub> (NH <sub>2</sub> pym) <sub>2</sub> (PPh <sub>3</sub> ) <sub>4</sub> (SO <sub>4</sub> )]·2CH <sub>3</sub> OH	2	4	μ <sub>1</sub> -N <sup>1</sup>	22
4	EXAXEH	<i>Pbca</i>	[Ag(NH <sub>2</sub> pym) <sub>2</sub> (PPh <sub>3</sub> ) <sub>2</sub> ]·BF <sub>4</sub>	1	3	μ <sub>1</sub> -N <sup>1</sup>	22
5	EXEMUQ	<i>P2</i> <sub>1</sub> / <i>c</i>	[Ag(Br-apym) <sub>2</sub> ]·CF <sub>3</sub> SO <sub>3</sub>	1	2	μ <sub>1</sub> -N <sup>1</sup>	23
6	EXENEB	<i>R</i> <sub>3</sub>	[Ag(Br-apym)(CF <sub>3</sub> SO <sub>3</sub> )] <sub>6</sub> ·6C <sub>4</sub> H <sub>10</sub>	6	2	μ <sub>2</sub> -N <sup>1</sup> :N <sup>1</sup>	23
7	HORWAN	<i>C2/c</i>	[Ag(ph-apym) <sub>2</sub> ]·BF <sub>4</sub>	1	2	μ <sub>1</sub> -N <sup>1</sup>	24
8	HORWER	<i>P2</i> <sub>1</sub> / <i>c</i>	[Ag(1-np-apym) <sub>2</sub> ]·BF <sub>4</sub>	1	2	μ <sub>1</sub> -N <sup>1</sup>	24
9	HORWIV	<i>P2</i> <sub>1</sub> / <i>c</i>	[Ag(2-np-apym) <sub>2</sub> ]·BF <sub>4</sub>	1	2	μ <sub>1</sub> -N <sup>1</sup>	24
10	LAFNIQ	<i>P</i> <sub>1</sub>	[Ag(NH <sub>2</sub> pym) <sub>2</sub> ]·AsF <sub>6</sub> ·NH <sub>2</sub> pym	1	2	μ <sub>1</sub> -N <sup>1</sup>	25
11	OJEDAJ	<i>P</i> <sub>1</sub>	[Ag <sub>2</sub> (dmoapym) <sub>3</sub> ]·2CF <sub>3</sub> SO <sub>3</sub>	2	2	μ <sub>1</sub> -N <sup>1</sup> and μ <sub>2</sub> -N <sup>1</sup> :N <sup>1</sup>	26
12	OPASEE	<i>P2</i> <sub>1</sub> / <i>m</i>	[Ag <sub>2</sub> (NH <sub>2</sub> pym) <sub>2</sub> (SO <sub>4</sub> )(dppm) <sub>2</sub> ]·CH <sub>3</sub> OH	2	4	μ <sub>1</sub> -N <sup>1</sup>	27
13	POGPUX	<i>P</i> <sub>1</sub>	[Ag <sub>4</sub> (NH <sub>2</sub> dmpym) <sub>6</sub> (NO <sub>3</sub> ) <sub>4</sub> ]	4	3 and 4	μ <sub>1</sub> -N <sup>1</sup> and μ <sub>2</sub> -N <sup>1</sup> :N <sup>1</sup>	28
14	RESDUP	<i>P4</i> <sub>2</sub> / <i>nmc</i>	[Ag(I-apym)]·NO <sub>3</sub> ·CH <sub>3</sub> CN	4	2	μ <sub>2</sub> -N <sup>1</sup> :N <sup>1</sup>	7
15	RUYKEC	<i>P</i> <sub>1</sub>	[Ag(NH <sub>2</sub> dmpym) <sub>2</sub> (ox) <sub>0.5</sub> ]·3H <sub>2</sub> O	2	2	μ <sub>1</sub> -N <sup>1</sup>	29
16	UMOCII	<i>P</i> <sub>1</sub>	[Ag(NH <sub>2</sub> pym) <sub>2</sub> ] <sub>2</sub> ·2CF <sub>3</sub> SO <sub>3</sub> ·H <sub>2</sub> O	2	2	μ <sub>1</sub> -N <sup>1</sup>	30
17	UYEJUE	<i>R</i> <sub>3</sub>	[Ag(I-apym)]·CF <sub>3</sub> SO <sub>3</sub>	6	2	μ <sub>2</sub> -N <sup>1</sup> :N <sup>1</sup>	23
18	YOKPUK	<i>P</i> <sub>1</sub>	[Ag <sub>2</sub> (NH <sub>2</sub> dmpym) <sub>4</sub> ]·2ClO <sub>4</sub>	2	3	μ <sub>1</sub> -N <sup>1</sup> and μ <sub>2</sub> -N <sup>1</sup> :N <sup>1</sup>	32
19	YUCYAX	<i>P2</i> <sub>1</sub> / <i>n</i>	[Ag(NH <sub>2</sub> pym) <sub>2</sub> ]·ClO <sub>4</sub>	1	2	μ <sub>1</sub> -N <sup>1</sup>	33
20	IZECUM	<i>P2</i> <sub>1</sub> / <i>c</i>	[Ag <sub>4</sub> (NHpym) <sub>2</sub> (dppm) <sub>2</sub> ]·2ClO <sub>4</sub> ·2DMF	4	2 and 3	μ <sub>3</sub> -N <sup>1</sup> :N <sup>2</sup> imino	34
21	KEXFUP	<i>P</i> <sub>1</sub>	[Ag <sub>2</sub> (dpypym-2) <sub>2</sub> ]·2NO <sub>3</sub>	2	3	μ <sub>1</sub> -N <sup>1</sup>	35
22	OKABOS	<i>P2</i> <sub>1</sub> / <i>c</i>	[Ag <sub>4</sub> (NHdmpym) <sub>2</sub> (dppm) <sub>2</sub> ]·4ClO <sub>4</sub>	4	2 and 3	μ <sub>2</sub> -N <sup>1</sup> :N <sup>1</sup> imino and μ <sub>3</sub> -N <sup>1</sup> :N <sup>2</sup> imino	36
23	UYEJIS	<i>P4</i> <sub>2</sub> / <i>nmc</i>	[Ag(Cl-apym)]·NO <sub>3</sub>	4	2	μ <sub>2</sub> -N <sup>1</sup> :N <sup>1</sup>	23
24	UYEJOY	<i>P4</i> <sub>2</sub> / <i>nmc</i>	[Ag(Br-apym)]·NO <sub>3</sub>	4	2	μ <sub>2</sub> -N <sup>1</sup> :N <sup>1</sup>	23
25	UYURAI	<i>P2</i> <sub>1</sub> / <i>c</i>	[Ag <sub>6</sub> (NHdmpym) <sub>2</sub> (dppm) <sub>4</sub> ]·4ClO <sub>4</sub>	6	3	μ <sub>4</sub> -N <sup>1</sup> :N <sup>1</sup> :N <sup>2</sup> imino	34

more pronounced growth of this research area in the near future, this review aims to consolidate the corresponding state-of-the-art knowledge and to attract attention toward the still limited use of NH<sub>2</sub>pym and its derivatives in the design of coordination architectures. The present review shows that NH<sub>2</sub>pym-based coordination architectures feature a high diversity of structural motifs and topologies that range from 0D metal-organic macrocycle compounds (Table 1), to linear, zigzag, double, triple 1D chains (Table 2) to flat, undulated, even entangled 2D layers (Table 3), as well as to 2D + 2D → 3D polycatenated network and other complicated 3D networks with diverse topologies (Table 4). Hence, more detailed descriptions of topologies and structural features of them are given below. The structural representations of selected examples were designed with Diamond software<sup>15</sup> using CIF files exported from the CSD.

### 3. NH<sub>2</sub>pym and its derivative based coordination architectures

#### 3.1. Synthesis considerations

The syntheses of these coordination compounds involve the reaction of NH<sub>2</sub>pym or its derivatives with different silver salts in elaborately selected solvents. The formed products are mainly crystals of high quality for X-ray diffraction characterization. The exploration for suitable reaction conditions by changing the solvents, anions, concentrations and ratios of the reactants is commonplace, which also usually determines the quality of obtained crystals of a coordination

compound for given components.<sup>16</sup> Although NH<sub>2</sub>pym and its derivatives are well soluble in a wide range of solvents and the silver salts also could be dissolved in many solvents, it is highly intractable that direct mixing of the two reactants leads often immediately to insoluble precipitates. To resolve this problem, decreasing the reaction speed between Ag(I) and ligand may be the only possible way. In general, three strategies have been widely adopted in the syntheses: (i) direct mixing of Ag(I) and ligand, then adding ammonia to get a clear solution under stirring or ultrasonic treatment; (ii) diffusion of a Ag(I) solution into a ligand solution by layering them on top of each other at room temperature; (iii) hydrothermal or solvothermal reaction<sup>17</sup> in a sealed tube or Teflon-lined reaction vessel at very high temperatures for a certain time, then slow cooling of the reaction system to form crystals. Among the three strategies, the first, ammonia-mediated assembly, is the most frequently encountered and very effective in synthesis of the crystalline Ag–NH<sub>2</sub>pym coordination compounds, despite that the NH<sub>3</sub> molecule usually does not participate in the final products. As we know, Ag(I) under ammoniacal conditions can form [Ag(NH<sub>3</sub>)<sub>2</sub>]<sup>n+</sup> (*n* = 1, 2 or 3)<sup>18</sup> which effectively reduces the reaction speed by slowly releasing the Ag(I) ions along with dissociation of NH<sub>3</sub> in dynamic equilibrium. This mechanism has long been known, but our group firstly exemplified this by capturing an intermediate which then transforms to a stable final compound in the mother liquor.<sup>19</sup> This observation not only offers important information on in-depth understanding of the self-assembly process involving Ag(I) under ammoniacal conditions but also justifies the effectiveness of the first strategy.

**Table 2** A summary of the 1D structures in this highlight

Complex	Refcode	Space group	Formula	Structure motif	Coordination number of Ag	Coordination mode of ligand	Ref.
26	GEZVOY	P2 <sub>1</sub> /c	[Ag(nfapym)ClO <sub>4</sub> ] <sub>n</sub>	Double-strands	4	$\mu_2\text{-N}^1:\text{N}^1$	40
27	GEZVUE	P2 <sub>1</sub> /c	[Ag(nfapym)CF <sub>3</sub> SO <sub>3</sub> ·EtOH] <sub>n</sub>	Zigzag chain	3	$\mu_2\text{-N}^1:\text{N}^1$	40
28	GEZWAL	C2/c	[Ag(nfapym)CF <sub>3</sub> CO <sub>2</sub> ] <sub>n</sub>	Zigzag chain	3	$\mu_2\text{-N}^1:\text{N}^1$	40
29	GEZVEO	C2/c	[Ag(nfapym)NO <sub>3</sub> ] <sub>n</sub>	Double-strands	4	$\mu_2\text{-N}^1:\text{N}^1$	40
30	GEZWUF	C2/c	[Ag(ofapym)CF <sub>3</sub> SO <sub>3</sub> ·EtOH] <sub>n</sub>	Zigzag chain	3	$\mu_2\text{-N}^1:\text{N}^1$	40
31	EPICEM	P1	[Ag <sub>2</sub> (NH <sub>2</sub> dmpym) <sub>4</sub> (mal)·H <sub>2</sub> O] <sub>n</sub>	Zigzag chain	4	$\mu_1\text{-N}^1$	41
32	EXAWOQ	P1	[Ag <sub>4</sub> (NO <sub>3</sub> ) <sub>4</sub> (PPh <sub>3</sub> ) <sub>4</sub> (NH <sub>2</sub> pym) <sub>2</sub> ] <sub>n</sub>	Zigzag chain	4	$\mu_2\text{-N}^1:\text{N}^1$	22
33	EXAWUW	P1	[Ag <sub>4</sub> (Ac) <sub>4</sub> (PPh <sub>3</sub> ) <sub>4</sub> (NH <sub>2</sub> pym) <sub>2</sub> ] <sub>n</sub>	Zigzag chain	5	$\mu_2\text{-N}^1:\text{N}^1$	22
34	EXEMOK	P2 <sub>1</sub> /c	[Ag(Cl-apym) <sub>2</sub> (CF <sub>3</sub> SO <sub>3</sub> ) <sub>n</sub> ]	Zigzag chain	3	$\mu_2\text{-N}^1:\text{N}^1$ <sub>amino</sub>	23
35	HAYWUB	P4/ncc	[Ag <sub>2</sub> (caapym) <sub>2</sub> (CH <sub>3</sub> CO <sub>2</sub> ) <sub>2</sub> ] <sub>n</sub>	Zigzag chain	2 and 4	$\mu_2\text{-N}^1:\text{N}^1$	42
36	HAYXAI	P4/ncc	[Ag <sub>2</sub> (caapym) <sub>2</sub> (CF <sub>3</sub> CO <sub>2</sub> ) <sub>2</sub> ] <sub>n</sub>	Zigzag chain	2 and 4	$\mu_2\text{-N}^1:\text{N}^1$	42
37	HAYXEM	P2/c	[Ag(caapym) <sub>2</sub> ] <sub>n</sub> ·nBF <sub>4</sub>	Linear chain	4	$\mu_2\text{-N}^1:\text{N}^1$ <sub>amino</sub>	42
38	HAYXIQ	P2/c	[Ag(caapym) <sub>2</sub> ] <sub>n</sub> ·nClO <sub>4</sub>	Linear chain	4	$\mu_2\text{-N}^1:\text{N}^1$ <sub>amino</sub>	42
39	KEXFID	C2/c	[Ag <sub>2</sub> (dpyapym-1) <sub>2</sub> ] <sub>n</sub> ·2nNO <sub>3</sub>	Linear chain	3	$\mu_2\text{-N}^1:\text{N}^1$	35
40	IGUGUN	C2/c	[Ag <sub>2</sub> (NH <sub>2</sub> pym) <sub>2</sub> (ox)]·2H <sub>2</sub> O	Ladder	3	$\mu_3\text{-N}^1:\text{N}^1:\text{N}^1$ <sub>amino</sub>	43
41	ILAFOR	P2 <sub>1</sub> /c	[Ag <sub>2</sub> (NH <sub>2</sub> dmpym) <sub>3</sub> (Hnta)] <sub>n</sub>	Zigzag chain	3 and 4	$\mu_1\text{-N}^1$	44
42	KEXFEZ	Pbca	[Ag(dpyapym-2)] <sub>n</sub> ·nCF <sub>3</sub> SO <sub>3</sub>	Linear chain	4	$\mu_2\text{-N}^1:\text{N}^1$	35
43	KEXFOJ	P2/c	[Ag <sub>2</sub> (dpyapym-2)(SCN) <sub>2</sub> ] <sub>n</sub> ·nH <sub>2</sub> O	Ladder	4	$\mu_2\text{-N}^1:\text{N}^1$	35
44	LURCUX	P1	[Ag <sub>4</sub> (NH <sub>2</sub> dmpym) <sub>4</sub> (pma)·(H <sub>2</sub> O) <sub>2</sub> ] <sub>n</sub> ·6nH <sub>2</sub> O	Fishbone	2 and 3	$\mu_1\text{-N}^1$	45
45	MAJLUF	P2 <sub>1</sub> /n	[Ag(NH <sub>2</sub> pym)(bza)] <sub>n</sub>	Linear chain	3	$\mu_2\text{-N}^1:\text{N}^1$	46
46	MUTJER	P1	[Ag <sub>4</sub> (NH <sub>2</sub> dmpym) <sub>6</sub> (butca)·2H <sub>2</sub> O] <sub>n</sub>	Linear chain	3	$\mu_1\text{-N}^1$	47
47	NUSNAQ	P2 <sub>1</sub> /n	[Ag <sub>2</sub> (pts) <sub>2</sub> (NH <sub>2</sub> pym) <sub>4</sub> ] <sub>n</sub>	Linear chain	3	$\mu_2\text{-N}^1:\text{N}^1$	14
48	NUSNEU	C2/c	[Ag <sub>2</sub> (pts) <sub>2</sub> (NH <sub>2</sub> dmpym) <sub>3</sub> ] <sub>n</sub>	Helical chain	4	$\mu_1\text{-N}^1$ , $\mu_2\text{-N}^1:\text{N}^1$	14
49	OJECUC	P2 <sub>1</sub> /c	[Ag <sub>2</sub> (NH <sub>2</sub> mompym) <sub>2</sub> (CF <sub>3</sub> SO <sub>3</sub> ) <sub>2</sub> ] <sub>n</sub>	Mixed anionic and cationic chain	2 and 4	$\mu_2\text{-N}^1:\text{N}^1$	26
50	OJEDEN	Pcnn	[Ag(dmoapym)(CF <sub>3</sub> CO <sub>2</sub> ) <sub>n</sub> ]	Zigzag chain	3	$\mu_2\text{-N}^1:\text{N}^1$	26
51	POGQAE	P2 <sub>1</sub> /n	[Ag(NH <sub>2</sub> pym)(NO <sub>3</sub> )] <sub>n</sub>	Zigzag chain	4	$\mu_2\text{-N}^1:\text{N}^1$	28
52	POGQEI	P2 <sub>1</sub> /c	[Ag(NH <sub>2</sub> mompym)(NO <sub>3</sub> )] <sub>n</sub>	Zigzag chain	5	$\mu_2\text{-N}^1:\text{N}^1$	28
53	POGQIM	C2/c	[Ag(dmoapym)(NO <sub>3</sub> )] <sub>n</sub>	Zigzag chain	3	$\mu_2\text{-N}^1:\text{N}^1$	28
54	QIGHOD	P2 <sub>1</sub> /c	[Ag(NH <sub>2</sub> pym)(bnb)] <sub>n</sub>	Linear chain	3	$\mu_2\text{-N}^1:\text{N}^1$	48
55	QUBKEE	P2 <sub>1</sub> /c	[Ag(NH <sub>2</sub> pym)(ida)] <sub>n</sub> ·nH <sub>2</sub> O	Ladder	4	$\mu_3\text{-N}^1:\text{N}^1:\text{N}^1$ <sub>amino</sub>	6
56	RESFAX	I4 <sub>1</sub> /a	[Ag(I-apym)(PF <sub>6</sub> ) <sub>n</sub> ]	Helical chain	2	$\mu_2\text{-N}^1:\text{N}^1$	7
57	RESFEB	Pnma	[Ag(I-apym)(ClO <sub>4</sub> ) <sub>n</sub> ]	Helical chain	2	$\mu_2\text{-N}^1:\text{N}^1$	7
58	UFAWAZ	C2/c	[Ag <sub>2</sub> Cl <sub>2</sub> (NH <sub>2</sub> pym)(Ph <sub>3</sub> P) <sub>2</sub> ] <sub>n</sub>	Linear chain	4	$\mu_2\text{-N}^1:\text{N}^1$	49
59	UNEKAA	P1	[Ag(fapym)(CO <sub>2</sub> CF <sub>3</sub> ) <sub>n</sub> ]	Linear chain	3	$\mu_2\text{-N}^1:\text{N}^1$	50
60	UNEKEE	C2/c	[Ag(fapym)(SO <sub>3</sub> CF <sub>3</sub> )·EtOH] <sub>n</sub>	Helical chain	4	$\mu_2\text{-N}^1:\text{N}^1$	50
61	UNEKII	P2 <sub>1</sub> /c	[Ag(fapym)(SO <sub>3</sub> CF <sub>3</sub> )· <sup>i</sup> PrOH] <sub>n</sub>	Helical chain	4	$\mu_2\text{-N}^1:\text{N}^1$	50
62	UNEKOO	P2 <sub>1</sub> /c	[Ag(fapym)(NO <sub>3</sub> )] <sub>n</sub>	Linear chain	3	$\mu_2\text{-N}^1:\text{N}^1$	50
63	UYEKAL	Ibca	[Ag(Cl-apym)(ClO <sub>4</sub> ) <sub>n</sub> ]	Helical chain	2	$\mu_2\text{-N}^1:\text{N}^1$	23
64	UYEKEP	Pbca	[Ag(Br-apym)(ClO <sub>4</sub> ) <sub>n</sub> ]	Helical chain	2	$\mu_2\text{-N}^1:\text{N}^1$	23
65	VECZAF	P2 <sub>1</sub> /c	[Ag(NH <sub>2</sub> dmpym)(NO <sub>3</sub> )] <sub>n</sub>	Helical chain	3 and 5	$\mu_2\text{-N}^1:\text{N}^1$	5
66	VECZEJ	P2 <sub>1</sub> /n	[Ag(NH <sub>2</sub> dmpym)(ClO <sub>4</sub> )·H <sub>2</sub> O] <sub>n</sub>	Zigzag chain	3	$\mu_2\text{-N}^1:\text{N}^1$	5
67	WUXJEF	P1	[Ag(NH <sub>2</sub> mompym)(26npd) <sub>0.5</sub> ·H <sub>2</sub> O] <sub>n</sub>	Fishbone	3	$\mu_1\text{-N}^1$	51
68	XULXAD	C2/c	[Ag <sub>2</sub> (NH <sub>2</sub> pym)(Ph <sub>3</sub> P) <sub>2</sub> ] <sub>n</sub>	Linear chain	4	$\mu_2\text{-N}^1:\text{N}^1$	52
69	YOKPIY	P1	[Ag <sub>4</sub> (NH <sub>2</sub> dmpym) <sub>4</sub> (CF <sub>3</sub> CO <sub>2</sub> ) <sub>4</sub> ] <sub>n</sub>	Ladder	4	$\mu_2\text{-N}^1:\text{N}^1$	32
70	YOKPOE	Pbca	[Ag(NH <sub>2</sub> dmpym)(CF <sub>3</sub> SO <sub>3</sub> )(H <sub>2</sub> O)] <sub>n</sub>	Linear chain	4	$\mu_2\text{-N}^1:\text{N}^1$	32
71	GUPXEV	C2/c	[Ag <sub>2</sub> (NH <sub>2</sub> pym) <sub>1.5</sub> (nipa)·H <sub>2</sub> O] <sub>n</sub>	Zigzag chain	2;3	$\mu_2\text{-N}^1:\text{N}^1$	54
72	YOKQEY	Pccn	[Ag(dmoapym)(ClO <sub>4</sub> ) <sub>n</sub> ]	Double strands	2	$\mu_2\text{-N}^1:\text{N}^1$	32
73	HOGCEM	P2 <sub>1</sub> /c	[Ag <sub>3</sub> (dmoapym) <sub>3</sub> (NO <sub>3</sub> ) <sub>3</sub> ] <sub>n</sub>	Triple strands	2 and 3	$\mu_1\text{-N}^1$ , $\mu_2\text{-N}^1:\text{N}^1$	28
74	EXENAX	P2 <sub>1</sub> /c	[Ag(I-apym)(CF <sub>3</sub> SO <sub>3</sub> ) <sub>n</sub> ]	Zigzag chain	3	$\mu_2\text{-N}^1:\text{N}^1$	23

In the synthesis of Ag/NH<sub>2</sub>pym/carboxylate coordination compounds, the selection of silver salt could determine whether the auxiliary anionic carboxylate ligand is incorporated in final products. Thus, Ag<sub>2</sub>O, not AgNO<sub>3</sub> or other common Ag(i) salts, was usually used in synthesis of Ag(i) mixed-ligand coordination compounds to promote the carboxylates instead of small anions to coordinate to the Ag(i) centers. Due to the insolubility of Ag<sub>2</sub>O, ammonia is indispensable during the assembly.

### 3.2. 0D coordination compounds

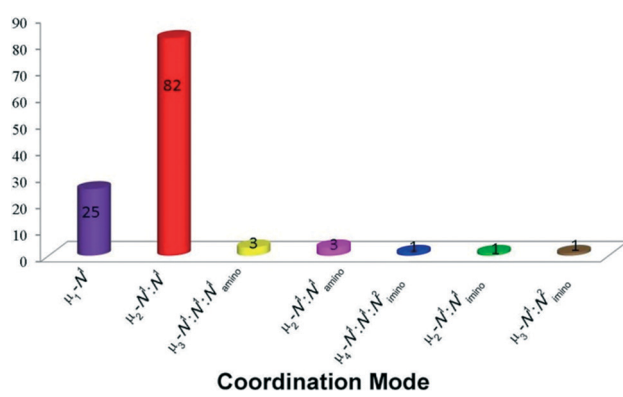
By analysis of 0D coordination compounds (1–25), we found that NH<sub>2</sub>pym or its derivatives were inclined to adopt  $\mu_1\text{-N}^1$  and  $\mu_2\text{-N}^1:\text{N}^1$  coordination mode, whereas the silver(i) ion generally displays linear, trigonal, and tetrahedral geometries, which led to diverse structures ranging from mono-, di-, tetra- and up to hexanuclear compounds. Due to the existence of amino group, uncoordinated heterocyclic N atom and anions, they could form different hydrogen bonds such

**Table 3** A summary of the 2D structures in this highlight

Complex	Refcode	Space group	Formula	Network topology	Coordination number	Coordination mode of ligand	Ref.
75	YOKQAR	<i>P</i> 2 <sub>1</sub> / <i>n</i>	[Ag(NH <sub>2</sub> mompym)(ClO <sub>4</sub> )] <sub>n</sub>	sql	4	μ <sub>2</sub> -N <sup>1</sup> :N <sup>1</sup>	32
76	GEZWOZ	<i>Pbc</i> a	[Ag(ofapym)ClO <sub>4</sub> ) <sub>n</sub>	sql	4	μ <sub>2</sub> -N <sup>1</sup> :N <sup>1</sup>	40
77	GEZXAM	<i>Pbc</i> a	[Ag(ofapym)CF <sub>3</sub> CO <sub>2</sub> ) <sub>n</sub>	hcb	4	μ <sub>2</sub> -N <sup>1</sup> :N <sup>1</sup>	40
78	GEZWIT	<i>P</i> 2 <sub>1</sub> / <i>c</i>	[Ag(ofapym)NO <sub>3</sub> ) <sub>n</sub>	sql	4	μ <sub>2</sub> -N <sup>1</sup> :N <sup>1</sup>	40
79	GEZVIS	<i>P</i> 2 <sub>1</sub> / <i>c</i>	[Ag(nfapym)NO <sub>3</sub> ) <sub>n</sub>	sql	4	μ <sub>2</sub> -N <sup>1</sup> :N <sup>1</sup>	40
80	GUPXIZ	<i>P</i> 2 <sub>1</sub> / <i>c</i>	[Ag <sub>2</sub> (NH <sub>2</sub> dmpym) <sub>2</sub> (nipa)] <sub>n</sub>	double layer	3	μ <sub>1</sub> -N <sup>1</sup> , μ <sub>2</sub> -N <sup>1</sup> :N <sup>1</sup>	54
81	FIJXON	<i>P</i> 1	[Ag <sub>2</sub> (NH <sub>2</sub> dmpym) <sub>2</sub> (26npd)] <sub>n</sub>	sql	4	μ <sub>2</sub> -N <sup>1</sup> :N <sup>1</sup>	55
82	AJIPOZ	<i>Pbc</i> a	[Ag(NH <sub>2</sub> dmpym)(NCS)] <sub>n</sub>	sql	4	μ <sub>2</sub> -N <sup>1</sup> :N <sup>1</sup>	56
83	BANMEK	<i>C</i> 2/ <i>c</i>	[Ag <sub>4</sub> (NH <sub>2</sub> pym) <sub>4</sub> (tcppta) <sub>2</sub> ] <sub>n</sub>	fes	2;4	μ <sub>2</sub> -N <sup>1</sup> :N <sup>1</sup>	57
84	BANMIO	<i>P</i> 1	[Ag <sub>2</sub> (NH <sub>2</sub> dmpym)(tcppta)] <sub>n</sub>	SP 2-periodic net (6,3)III	3	μ <sub>2</sub> -N <sup>1</sup> :N <sup>1</sup>	57
85	EPICAI	<i>Pca</i> 2 <sub>1</sub>	[Ag <sub>3</sub> (NH <sub>2</sub> pym) <sub>3</sub> (mal)NO <sub>3</sub> ) <sub>n</sub>	Pillared bilayer	4,5	μ <sub>2</sub> -N <sup>1</sup> :N <sup>1</sup>	41
86	ILAFIL	<i>Pcc</i> n	[{(NH <sub>4</sub> )Ag <sub>2</sub> (NH <sub>2</sub> mpty)(nta)-3H <sub>2</sub> O] <sub>n</sub>	10 <sup>3</sup>	3;4	μ <sub>2</sub> -N <sup>1</sup> :N <sup>1</sup>	44
87	LALDIN	<i>C</i> 2/ <i>c</i>	[Ag <sub>2</sub> (NH <sub>2</sub> dmpym) <sub>2</sub> (suc)-H <sub>2</sub> O] <sub>n</sub>	2D + 2D → 2D	2;4	μ <sub>2</sub> -N <sup>1</sup> :N <sup>1</sup>	58
88	MUTJAN	<i>P</i> 1	{[Ag <sub>4</sub> (NH <sub>2</sub> mpty) <sub>2</sub> (butca)(H <sub>2</sub> O) <sub>4</sub> ]·2H <sub>2</sub> O} <sub>n</sub>	sql	2;3	μ <sub>2</sub> -N <sup>1</sup> :N <sup>1</sup>	47
89	OKOVOA	<i>P</i> 2 <sub>1</sub> / <i>n</i>	[Ag(NH <sub>2</sub> pym)(nds) <sub>0.5</sub> ] <sub>n</sub>	sql	3	μ <sub>2</sub> -N <sup>1</sup> :N <sup>1</sup>	59
90	OKOVUG	<i>P</i> 2 <sub>1</sub> / <i>c</i>	[Ag(NH <sub>2</sub> dmpym)(nds) <sub>0.5</sub> ] <sub>n</sub>	sql	3	μ <sub>2</sub> -N <sup>1</sup> :N <sup>1</sup>	59
91	OPANEZ	<i>C</i> 2/ <i>c</i>	[Ag(NH <sub>2</sub> dmpym)(tpa) <sub>1/2</sub> ] <sub>n</sub>	sql	4	μ <sub>2</sub> -N <sup>1</sup> :N <sup>1</sup>	60
92	RUYJIF	<i>P</i> 2/ <i>c</i>	[Ag(NH <sub>2</sub> mpty)(suc) <sub>0.5</sub> ·0.5H <sub>2</sub> O] <sub>n</sub>	2D + 2D → 2D	2;4	μ <sub>2</sub> -N <sup>1</sup> :N <sup>1</sup>	29
93	RUYJOL	<i>P</i> 1	[Ag <sub>2</sub> (NH <sub>2</sub> mpty) <sub>2</sub> (glu) <sub>3</sub> ·1.5H <sub>2</sub> O] <sub>n</sub>	sql	3	μ <sub>2</sub> -N <sup>1</sup> :N <sup>1</sup>	29
94	RUYKAY	<i>P</i> 1	[Ag <sub>2</sub> (NH <sub>2</sub> mpty) <sub>2</sub> (tpa)(H <sub>2</sub> O)] <sub>n</sub>	sql	3;4	μ <sub>2</sub> -N <sup>1</sup> :N <sup>1</sup>	29
95	RUYKIG	<i>C</i> 2/ <i>c</i>	[Ag(NH <sub>2</sub> dmpym)(bbdc) <sub>0.5</sub> ·0.5H <sub>2</sub> O] <sub>n</sub>	sql	2;4	μ <sub>2</sub> -N <sup>1</sup> :N <sup>1</sup>	29
96	VECYOS	<i>P</i> 2 <sub>1</sub> 2 <sub>1</sub> 2 <sub>1</sub>	[Ag(NH <sub>2</sub> pym) <sub>1.5</sub> (ClO <sub>4</sub> )] <sub>n</sub>	hcb	3	μ <sub>2</sub> -N <sup>1</sup> :N <sup>1</sup>	5
97	VECYUY	<i>Ibam</i>	[Ag(NH <sub>2</sub> pym)(OAc)·2H <sub>2</sub> O] <sub>n</sub>	sql	3	μ <sub>2</sub> -N <sup>1</sup> :N <sup>1</sup>	5
98	VECZIN	<i>P</i> 2 <sub>1</sub> / <i>c</i>	[Ag <sub>4</sub> (NH <sub>2</sub> dmpym) <sub>2</sub> (SO <sub>4</sub> ) <sub>2</sub> (H <sub>2</sub> O) <sub>4</sub> ] <sub>n</sub>	sql	4	μ <sub>2</sub> -N <sup>1</sup> :N <sup>1</sup>	5
99	VIQQIX	<i>P</i> 1	[Ag <sub>3</sub> (NH <sub>2</sub> pym) <sub>3</sub> (stp)] <sub>n</sub> ·2nH <sub>2</sub> O	4, 4L34	3	μ <sub>2</sub> -N <sup>1</sup> :N <sup>1</sup>	61
100	VIJSOY	<i>P</i> 2 <sub>1</sub> / <i>c</i>	[Ag <sub>2</sub> (NH <sub>2</sub> dmpym) <sub>2</sub> (Hstp)(H <sub>2</sub> O)] <sub>n</sub> ·nH <sub>2</sub> O	sql	3;4	μ <sub>2</sub> -N <sup>1</sup> :N <sup>1</sup>	61

**Table 4** A summary of the 3D structures in this highlight

Complex	Refcode	Space group	Formula	Network topology	Coordination number	Coordination mode of ligand	Ref.
101	ILAFEH	<i>P</i> 2 <sub>1</sub> / <i>m</i>	[Ag <sub>1.5</sub> (NH <sub>2</sub> pym)(nta) <sub>0.5</sub> ] <sub>n</sub>	—	3	μ <sub>2</sub> -N <sup>1</sup> :N <sup>1</sup>	44
102	LAUDOT	<i>P</i> 2 <sub>1</sub> / <i>n</i>	[Ag <sub>2</sub> (NH <sub>2</sub> dmpym) <sub>2</sub> (ipa)-2H <sub>2</sub> O] <sub>n</sub>	2D + 2D → 3D	2;4	μ <sub>2</sub> -N <sup>1</sup> :N <sup>1</sup>	58
103	RUYJUR	<i>P</i> 2 <sub>1</sub> / <i>c</i>	[Ag <sub>2</sub> (NH <sub>2</sub> mpty) <sub>2</sub> (ipa)-2H <sub>2</sub> O] <sub>n</sub>	2D + 2D → 3D	2;4	μ <sub>2</sub> -N <sup>1</sup> :N <sup>1</sup>	29
104	AJIPUF	<i>Pbc</i> n	[Ag <sub>2</sub> (NH <sub>2</sub> pym)(NCS)] <sub>n</sub>	nce	4	μ <sub>2</sub> -N <sup>1</sup> :N <sup>1</sup>	56
105	VECYIM	<i>C</i> 2/ <i>c</i>	[Ag <sub>2</sub> (NH <sub>2</sub> pym) <sub>2</sub> (SO <sub>4</sub> )] <sub>n</sub>	vmd	4	μ <sub>3</sub> -N <sup>1</sup> :N <sup>1</sup> :N <sup>1</sup> amino	5
106	OPANAV	<i>R</i> 3	[Ag(NH <sub>2</sub> dmpym)(btc) <sub>1/3</sub> ] <sub>n</sub>	loh1	4	μ <sub>2</sub> -N <sup>1</sup> :N <sup>1</sup>	60
107	IGUHAU	<i>C</i> 2/ <i>c</i>	[Ag <sub>2</sub> (NH <sub>2</sub> pym) <sub>2</sub> (glu)]·H <sub>2</sub> O	osb/Cmcm-C2/c	3	μ <sub>2</sub> -N <sup>1</sup> :N <sup>1</sup>	43
108	IGUHEY	<i>P</i> nna	[Ag <sub>2</sub> (NH <sub>2</sub> pym) <sub>2</sub> (14npd)]·2H <sub>2</sub> O	dia	4	μ <sub>2</sub> -N <sup>1</sup> :N <sup>1</sup>	43
109	GUKQIN	<i>P</i> 1	[Ag <sub>3</sub> (NH <sub>2</sub> pym) <sub>2</sub> (btc)] <sub>n</sub>	—	3	μ <sub>2</sub> -N <sup>1</sup> :N <sup>1</sup>	71
110	LURCOR	<i>P</i> 1	[Ag <sub>4</sub> (NH <sub>2</sub> pym) <sub>2</sub> (pma)-(H <sub>2</sub> O) <sub>2</sub> ] <sub>n</sub>	—	2;4	μ <sub>2</sub> -N <sup>1</sup> :N <sup>1</sup>	45

**Scheme 3** A schematic comparison of amounts of coordination species involving 2-aminopyrimidine with different binding modes.

as complementary N<sub>amino</sub>-H···N<sub>heterocycle</sub>, N<sub>amino</sub>-H···O<sub>anion</sub>, and N<sub>amino</sub>-H···F<sub>anion</sub> to stabilize themselves in crystal lattices.<sup>31</sup> The structure motifs of 0D coordination compounds are listed in Table 1. Among them, several interesting anion-dependent metallamacrocyclic coordination compounds were reported by Chen's group. One-pot reaction of AgNO<sub>3</sub> and 2-amino-5-halopyrimidine in CH<sub>3</sub>CN or THF then growth of single crystals by diffusion gave compounds 14, 23, and 24 as an interesting saddle-shaped motif. They are constructed from four Ag(I) atoms and four μ<sub>2</sub>-N<sup>1</sup>:N<sup>1</sup> 2-amino-5-halopyrimidine ligands, giving a 16-membered metal-organic macrocycle (Fig. 1a).<sup>7,23</sup> Due to weak coordination effects of the NO<sub>3</sub><sup>-</sup> ion, the central Ag(I) atoms coordinate to N atoms in a bend fashion (N-Ag-N angles: 144.3, 151.4 and 148.9° for 14, 23, and 24) instead of a perfect linear fashion, which is responsible to the formation of cyclic structures. When using

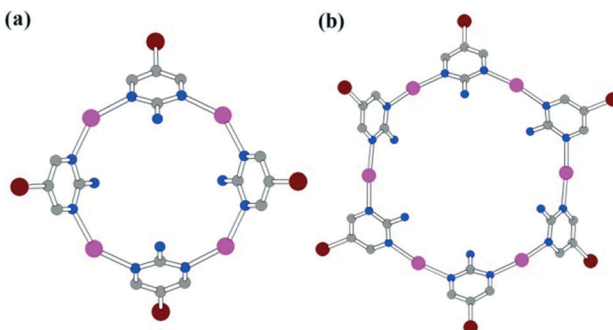


**Fig. 1** (a) The 16-membered metal-organic macrocycle in tetranuclear 14. (b) The 24-membered metal-organic macrocycle in hexanuclear 17. (Purple ball: Ag; gray ball: C; blue ball: N; brown ball: I).

a similar method but larger  $\text{CF}_3\text{SO}_3^-$ , a larger 24-membered metal-organic macrocycle (Fig. 1b) comprising six  $\text{Ag}(\text{i})$  atoms and six  $\mu_2\text{N}^1:\text{N}^1$  2-amino-5-halopyrimidine ligands in compounds 6 and 17 was observed.<sup>23</sup> Compared to the 16-membered metal-organic macrocycle in 14, 23, and 24, the coordinative tension around the  $\text{Ag}(\text{i})$  atom was released with a larger N–Ag–N angle of *ca.* 164°. Many kinds of supramolecular interactions such as halogen bonding, hydrogen bonding and aromatic packing were observed in them.

In this family, our group firstly found the rare coordination modes of  $\text{NH}_2\text{pym}$  and  $\text{NH}_2\text{dmpym}$ ,  $\mu_3\text{N}^1:\text{N}^2_{\text{imino}}$  and  $\mu_4\text{N}^1:\text{N}^1:\text{N}^2_{\text{imino}}$  in mixed-ligand tetranuclear 20 and hexanuclear 25 (Fig. 2a and b),<sup>34</sup> which were obtained in strong base solution (pH high up to ~13) caused by  $\text{Ag}_2\text{O}$  and ammonia. The bidentate bridging dppm ligand combines the  $\text{NH}_2\text{pym}$  or  $\text{NH}_2\text{dmpym}$  ligands to give 20 and 25 rectangle  $\text{Ag}_4$  and triangle  $\text{Ag}_3$  cores, respectively. The  $\text{NH}_2\text{dmpym}$  uses another heterocyclic N atom to bind the  $\text{Ag}_3$  core to the overall hexanuclear motif in 25. The  $\text{Ag}\cdots\text{Ag}$  distances fall in the range of 2.8852(15)–3.3202(13) Å and 3.0362(9)–3.1721(8) Å for 20 and 25, respectively, which are obviously shorter than twice the van der Waals radius for silver atoms (3.44 Å), indicating important argentophilic interaction proved to influence the structures of supramolecular assemblies as well as related properties such as photoluminescence and conduction, and their importance has been crystallographically and theoretically documented.

As we know, the  $\text{Ag}-\text{N}_{\text{pyrimidyl}}$  distances should be shorter than that of  $\text{Ag}-\text{N}_{\text{amino}}$  which is partially due to the

dissimilarity of electric effects between amino and pyrimidyl N atoms. But in these two cases, each amino group loses one H atom to form an electronegative imino group which causes the  $\text{N}_{\text{imino}}$  to be a stronger electronic donor to  $\text{Ag}(\text{i})$  than  $\text{N}_{\text{pyrimidyl}}$ . In 20,  $\text{Ag}-\text{N}_{\text{imino}}$  bonds are a shorter and a longer one, (2.113(5) and 2.534(5) Å) which indicates the unequal coordination behaviors between the lone-pair electron and negative charge of  $\text{N}_{\text{imino}}$  on  $\text{NH}_2\text{pym}$ . In 25, both  $\text{Ag}-\text{N}_{\text{imino}}$  bonds are shorter ones (2.194(6) and 2.161(5) Å) which indicates that the lone-pair electron and negative charge of  $\text{N}_{\text{imino}}$  have the nearly equal ability of binding  $\text{Ag}(\text{i})$  ions and are delocalized to some extent. Although the  $\text{pK}_a$  value of the exocyclic amino group is high (20.5),<sup>37</sup> metal coordination effects can dramatically increase the acidity of protons, as a consequence, a more acidic amino group is generated which makes the formation of the imine anion to be facile and enables a second metal to bind at this site. In combination with the endocyclic N atoms, rare  $\mu_3$  or  $\mu_4$ -binding modes of the aminopyrimidyl ligands are *in situ* generated in this system.

In our following work,<sup>38</sup> we have carried a series of experiments to fully investigate the deprotonation mechanism. In nature, their rare coordination modes are realized by the deprotonation of the amino group which involves a metal-mediated N–H activation process in a strong base environment. The  $\text{pK}_a$  value of the exocyclic amino group is very high, so N–H activation of  $\text{NH}_2\text{pym}$  or  $\text{NH}_2\text{dmpym}$  is an extremely difficult task, especially in proton solvent systems containing water. We thus propose a synergistical activation process that the reaction undergoes a metal-coordination-mediated deprotonation process involving the transition state illustrated in Scheme 4. In comparison to the endocyclic N atom, the coordination ability of the exocyclic N atom is largely weakened due to the delocalization of a pair of lone electrons on p orbitals of the amino group towards the aromatic pyrimidyl ring. So, one possible transition state is a tridentate coordinated  $\text{NH}_2\text{pym}$  ligand with two strong  $\text{Ag}-\text{N}_{\text{pyrimidyl}}$   $\sigma$  bonds and one weak  $\text{Ag}-\text{N}_{\text{amino}}$   $\pi$  bond. This intermediate is dynamic and quickly releases its excess energy to transform to the resultant thermodynamic product by removal of  $\text{H}^+$  from the  $\text{NH}_2$  group under basic conditions to yield  $\text{NH}_2\text{pym}^-$  and water. Once the  $\text{NH}_2\text{pym}^-$  formed, the weak  $\text{Ag}-\text{N}_{\text{amino}}$   $\pi$  bond immediately isomerised to the strong  $\text{Ag}-\text{N}_{\text{imino}}$   $\sigma$  bond from the perpendicular direction with respect to pyrimidyl plane to the parallel direction. This mechanism also involved dearomatization of  $\text{NH}_2\text{pym}$ , following this, the aromatization of  $\text{NH}_2\text{pym}$  occurred with the

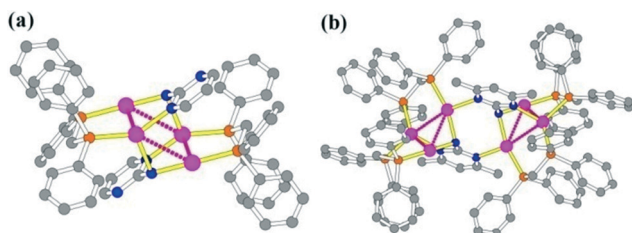
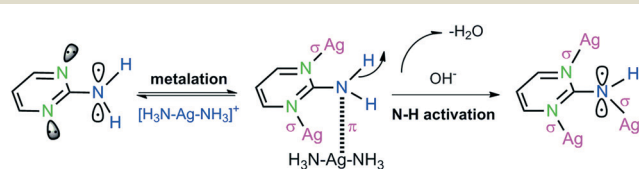


**Fig. 2** Molecular structure of tetranuclear 20 (a) and hexanuclear 25 (b). (Purple ball: Ag; blue ball: N; gray ball: C; orange ball: P).



**Scheme 4** The N–H activation mechanism in deprotonated  $\text{NH}_2\text{pym}$  ligand.

transformation of weak Ag–N<sub>amino</sub>  $\pi$  bond to strong Ag–N<sub>imino</sub>  $\sigma$  bond.

### 3.3. 1D coordination chain

The Ag(i) is found in a wide range of coordination environments: two-coordinated linearity, three-coordinated triangle, four-coordinated tetrahedron or planar square, five-coordinated square-pyramid and six-coordinated octahedron. According to previous summarized silver coordination geometry,<sup>39</sup> about a quarter of all silver coordination compounds are linear two-coordinated. Linear coordination geometry prefers to form 1D motifs. In our reviewed 110 compounds, nearly 50% are diverse 1D motifs.

Mattay's group used 5-polyfluoroarene-2-aminopyrimidine as a ligand to obtain a series of 1D Ag(i) coordination polymers with different counteranions (26–30 and 59–62).<sup>40,50</sup> Compound 26 showed double-strands bridged by an  $\mu_2$ -O:O<sup>−</sup>ClO<sub>4</sub><sup>−</sup> anion (Fig. 3a). The organic ligands uniformly direct to one side in each single strand. The non-coordinated oxygen atom of ClO<sub>4</sub><sup>−</sup> forms hydrogen bonding with the amino group. No Ag(i)···Ag(i) interaction was observed due to a long distance between adjacent Ag(i) atoms. The dihedral angle between parent NH<sub>2</sub>pym and F-substituted aryl is 35°, whereas the pyrimidyl ring and the NMe<sub>2</sub> group are almost coplanar (dihedral angle: 5.4°). When the anion was changed to CF<sub>3</sub>SO<sub>3</sub><sup>−</sup>, the zigzag chain was obtained for 27 (Fig. 3b). The central Ag(i) atom is located in a distorted trigonal geometry with the largest bond angle of 129°. The CF<sub>3</sub>SO<sub>3</sub><sup>−</sup> is hydrogen-bonded to the OH-group of the ethanol and amino group of parent NH<sub>2</sub>pym. The dihedral angles between the

pyrimidyl ring and the NMe<sub>2</sub> group are 87.3°, which is much larger than that in 26. When CF<sub>3</sub>CO<sub>2</sub><sup>−</sup> was used, a similar chain 28 with head-to-head arranged 5-polyfluoroarene-2-aminopyrimidine ligands was obtained (Fig. 3c). A ligand-unsupported Ag(i)···Ag(i) interchain distance of 3.049(5) Å is found. Compound 29 is also double-stranded, but 5-polyfluoroarene-2-aminopyrimidine ligands in each single strand of 29 are alternately arranged in a head-to-tail fashion (Fig. 3d). Two adjacent strands are bound together by a pair of centrosymmetric  $\mu_2$ -O:O NO<sub>3</sub><sup>−</sup> ions to give a double strand. The strand extends in a linear way parallel to the *c* axis. If the NMe<sub>2</sub> group was changed to OMe and the anion is CF<sub>3</sub>SO<sub>3</sub><sup>−</sup>, compound 30 was obtained being very similar to 27 (Fig. 3e). Although the coordination number in 26–30 is 3 or 4, the third or fourth coordination sites are usually weakly bound anions or solvent, which does not influence the resultant 1D motif.

His group also synthesized 2-amino-5-pentafluorophenylpyrimidine (fapym) and used it to assemble with diverse silver salts, giving compounds 59–62. All of them are single stranded, but the fapym ligands show a different orientation in the strand depending on which anion is presented in the lattice. Only when CF<sub>3</sub>CO<sub>2</sub><sup>−</sup> is presented, the fapym ligands in 59 are head-to-tail arranged in strands, where a head-to-head orientation of fapym was observed in 60–62.

Another interesting 1D motif was reported in compound 49<sup>26</sup> which consists of independently cationic [Ag(NH<sub>2</sub>mompym)]<sup>+</sup> (Fig. 4a) and anionic chains [Ag(NH<sub>2</sub>mompym)(CF<sub>3</sub>SO<sub>3</sub>)<sub>2</sub>]<sup>−</sup> (Fig. 4b). In the [Ag(NH<sub>2</sub>mompym)]<sup>+</sup> chain, the silver ion is coordinated by two pyrimidyl nitrogen atoms of two NH<sub>2</sub>mompym ligands in a distorted linear geometry. The charge balance was finished by another 1D anionic chain [Ag(NH<sub>2</sub>mompym)(CF<sub>3</sub>SO<sub>3</sub>)<sub>2</sub>]<sup>−</sup>, in which the central silver is coordinated by two oxygen atoms from two CF<sub>3</sub>SO<sub>3</sub><sup>−</sup> anions and two nitrogen atoms from two NH<sub>2</sub>mompym ligands in a distorted tetrahedral geometry. Intramolecular hydrogen bonds are observed in the anionic chain, involving the amino groups with the oxygen atoms on the coordinated CF<sub>3</sub>SO<sub>3</sub><sup>−</sup> anions. The rare structural feature of 49 is independent of the cationic and anionic chains which cross over with each other (Fig. 4c). No direct coordination bond

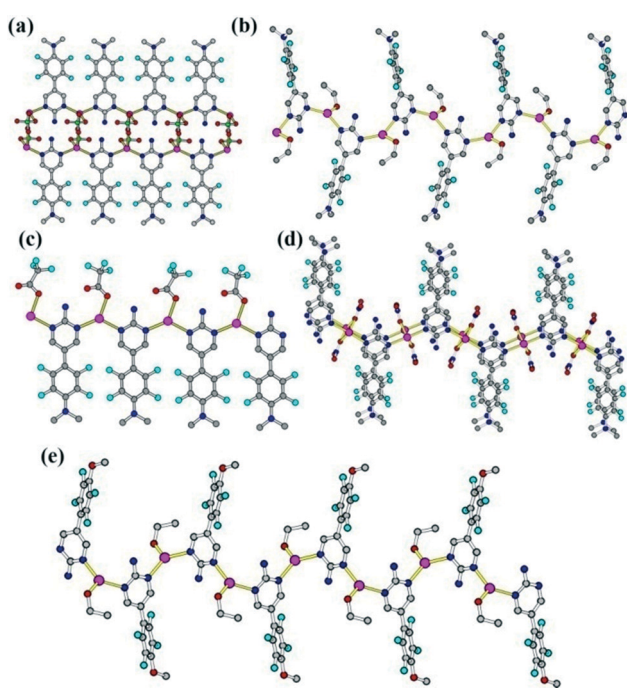


Fig. 3 1D chain structure of 26 (a), 27 (b), 28 (c), 29 (d) and 30 (e). (Purple ball: Ag; blue ball: N; gray ball: C; green ball: Cl; cyan ball: F).

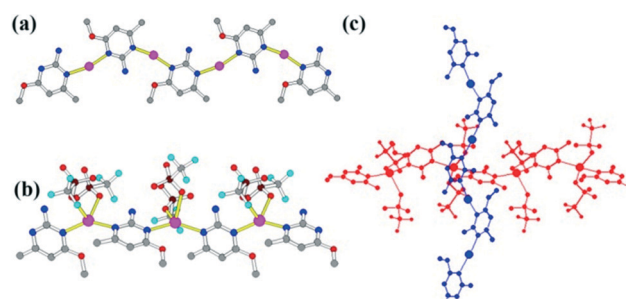


Fig. 4 The 1D cationic [Ag(NH<sub>2</sub>mompym)]<sup>+</sup> (a) and anionic chain [Ag(NH<sub>2</sub>mompym)(CF<sub>3</sub>SO<sub>3</sub>)<sub>2</sub>]<sup>−</sup> (b) in 49. (c) The crossover orientation of two independent chains. (Purple ball: Ag; blue ball: N; gray ball: C; brown ball: S; cyan ball: F).

between the two chains was found and only N-H $\cdots$ O intermolecular hydrogen bonds existed, where the O atoms of triflate anions from anionic chains act as acceptors while the N atom of the amino group from cation chains serves as donors. To the best of our knowledge, most of the reported 1D chains are single and neutral and some polymeric complexes containing two kinds of chains have been reported, however, the chains are usually not independent but are connected by coordination bonds.<sup>53</sup>

Another kind of representative 1D motif is the helical chain. In 46 1D structures, only five helical chains were found. Compounds 56 and 57 are a pair of anion-controlled helical structures. Compound 56 was solved in tetragonal space group  $I4_1/a$  and the Ag(i) atoms are bridged by the I-apym ligands to form a 1D helical chain along the  $4_1$  axis with  $\text{PF}_6^-$  as the counteranion (Fig. 5a and b).<sup>7</sup> The coordination geometry around Ag(i) is approximately 2-coordinated linearity with a N-Ag-N angle of 174°, and the dihedral angle between the two nearest pyrimidyl rings is 98°. The helical pitch of the repeating subunit involving five silver atoms and four ligands is 22.584 Å, equal to the length of the  $c$  axis. Noticeably, the helical chains are interlinked extensively through the unique discrete Ag $\cdots$ I (3.68 Å) and I $\cdots$ I (4.19 Å) interactions to form a 3D porous structure. The  $\text{PF}_6^-$  ions weakly interact with the metal center through long Ag $\cdots$ F (3.04–3.09 Å) distances. Compound 57 was crystallized in orthorhombic space group  $Pnma$  and with  $\text{ClO}_4^-$  as the counter-anion.<sup>7</sup> Both Ag(i) centers are coordinated by two N atoms of I-apym ligands. Two bond angles around Ag(i) centers are 178.9(4)° and 145.0(4)°. The latter small bond angle may be caused by adjacent  $\text{ClO}_4^-$  which weakly interacts with the Ag(i) center (2.93–3.34 Å). The formation of the 1D helical chain structure is associated with the dihedral angles between the two pyrimidyl rings coordinated to Ag(i) centers (3.1 and 56.7°). The helical pitch, defined by the distance between equivalent atoms generated by one full rotation of the crystallographic  $2_1$  screw axis, is 11.465 Å, which is equal to the  $b$ -axis length (Fig. 5c and d). The repeating unit of the

helical chain involves five silver atoms and four ligands. The adjacent helical chains are also interlinked through Ag $\cdots$ I and I $\cdots$ I interactions.

Chen's group also assembled Cl-apym and Br-apym with  $\text{AgClO}_4$  by liquid–liquid diffusion to give compounds 63 and 64. Both structures of 63 and 64 were solved in the orthorhombic space groups  $Ibca$  and  $Pbca$ , respectively.<sup>23</sup> While the asymmetric unit of 63 comprises two independent Ag(i) centers both with half occupancy, one Cl-apym ligand, and two independent half occupancy  $\text{ClO}_4^-$  anions. There are two Ag(i) centers, two Br-apym ligands and two  $\text{ClO}_4^-$  anions in 64. In them, one of the two independent Ag(i) atoms adopts a nearly linear geometry, but the other adopts a severely bent geometry with corresponding N-Ag-N angles of 172.4(3) and 138.3(3)° for 63 and 173.5(2) and 136.8(2)° for 64. The non-flat but twist conformations of two pyrimidyl rings around the same Ag(i) atom are observed with the dihedral angles between them being 51.2 and 6.0° in 63 and 50.2 and 5.3° in 64. Due to the dictation from bond angle and coordination conformation, the Ag(i) atoms in them are bridged by the Cl- or Br-apym pyrimidyl ligands to form 1D helical chains. The helical pitch values involving five silver atoms and four ligands are 7.15 and 7.20 Å for 63 and 64, respectively (Fig. 6).

They also used two methyl substituted  $\text{NH}_2\text{pym}$  ligands to construct a helical chain, 65, which crystallized in monoclinic space group  $P2_1/c$  with two independent  $\text{NO}_3^-$  as counteranions. One  $\text{NO}_3^-$  anion is coordinated to the Ag(i) atom in a monodentate fashion, whereas the other is in a bidentate fashion, which gives the Ag(i) atoms two types of coordination geometries. The bidentate  $\text{NH}_2\text{dmpym}$  ligand links Ag(i) atoms into the 1D helical chain (Fig. 7a and b). The repeating unit of the helical chain involves five silver atoms and four  $\text{NH}_2\text{dmpym}$  ligands and the helical pitch is 19.287 Å, equal to the length of the  $b$  axis. The single-stranded helical chain is interlinked through a series of Ag $\cdots$ O interactions (2.666(4) and 2.709(6) Å), forming the resulting 2D molecular layer.

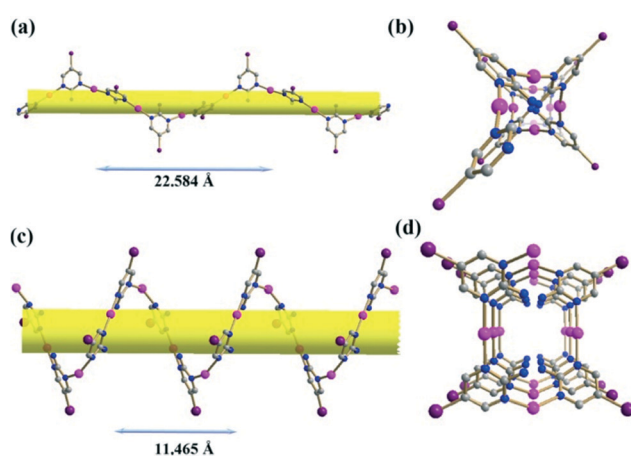


Fig. 5 The 1D helical chain for 56 (a and b) and 57 (c and d) viewed from different directions. (Purple ball: Ag; blue ball: N; gray ball: C; dark purple ball: I).

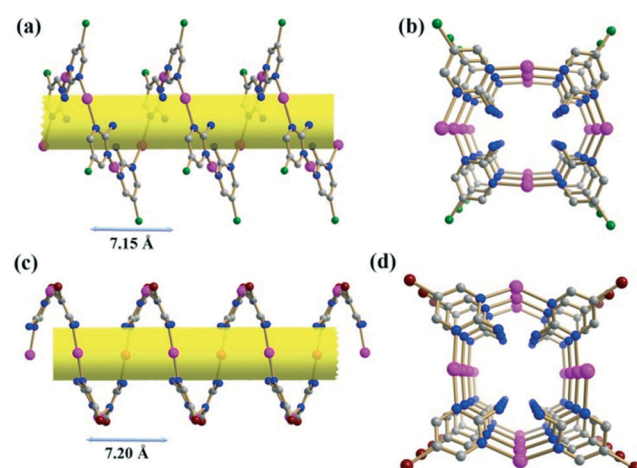
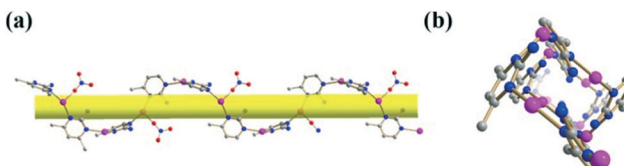


Fig. 6 The 1D helical chain for 63 (a and b) and 64 (c and d) viewed from different directions. (Purple ball: Ag; blue ball: N; gray ball: C; green ball: Cl; brown ball: Br).



**Fig. 7** The 1D helical chain for **65** viewed from different directions (a and b). (Purple ball: Ag; blue ball: N; gray ball: C).

In the 1D structure family, there are also many mixed-ligand coordination compounds, such as **31**, **41**, **44**, **46** and **67**, which usually contain monodentate coordinated  $\text{NH}_2\text{pym}$  or its derivatives but multidentate carboxylate ligands. The latter kind of ligand plays important roles in the construction of the 1D motif, whereas the monodentate coordinated  $\text{NH}_2\text{pym}$  or its derivatives form complementary  $\text{N}_{\text{amino}}\text{--H}\cdots\text{N}_{\text{heterocycle}}$  hydrogen bonds with adjacent chains. This suggests that suitable adjustment of the reaction conditions or modification of the ligand may enhance the N ligand bridging ability, so as to produce higher dimensional structures.

### 3.3. 2D layer

Among 110 silver(I)-2-aminopyrimidyl coordination architectures, 26 compounds are 2D layered structure motifs, and most of them (68%) are  $4^4\text{-sql}$  topological networks. Two compounds show interesting  $2\text{D} + 2\text{D} \rightarrow 2\text{D}$  parallel interpenetration topology.

Mattay's group showed that the polyfluoroarene-2-amino-pyrimidine also could be used to obtain a series of 2D  $\text{Ag}^{(1)}$  coordination layers modulated by anions (**76–79**).<sup>40</sup> All of them are built from anion-bridged  $\text{Ag}$ -ofapym or  $\text{Ag}$ -nfapym polymeric chains. The coordination modes of  $\text{ClO}_4^-$ ,  $\text{CF}_3\text{CO}_2^-$ , and  $\text{NO}_3^-$  are  $\mu_2\text{-O:O}$ ,  $\mu_2\text{-O:O}'$ ,  $\mu_2\text{-O:O}'$ , respectively. In the chain of **76**, the fluoroarene tail points to the same direction and forms weak  $\pi\cdots\pi$  interaction (centroid distance: 3.70 Å)<sup>62</sup> with fluoroarene of the adjacent chain. In **77**, the fluoroarene tail arranges toward the same direction, giving parallel alignment of the ligands. The  $\text{CF}_3\text{CO}_2$  bridge brings a pair of  $\text{Ag}(\text{i})$  ions in adjacent chains with a distance of 3.357(2) Å which is a little closer than the doubled van der Waals (vdW) radius of silver, indicating important argentophilicity.<sup>63</sup> Both structures of **77** and **78** are assembled by strands of ofapym or nfapym ligands in head-to-head alignment and bridging  $\mu_2\text{-O:O}'$  nitrate anions in an *anti-anti* fashion. Bridging anions play important roles in the formation of 2D layer structures. From a topology viewpoint, no polynuclear SBU (secondary building unit) was found in them and each  $\text{Ag}(\text{i})$  ion in **76**, **78**, and **79** is in 4-connected node which links its nearest four neighbors, giving them  $4^4\text{-sql}$  networks with different undulation degrees, whereas the  $\text{Ag}(\text{i})$  ion in **77** is in 3-connected node which links its nearest three neighbors, giving it a  $6^3\text{-hcb}$  network (Fig. 8).

Complex **80** possesses a double layer structure in which  $\text{NH}_2\text{dmpym}$  ligands show two different coordination modes,  $\mu_1\text{-N}^1$  and  $\mu_2\text{-N}^1:\text{N}^1$ . Two unique  $\text{Ag}(\text{i})$  ions adopt distorted

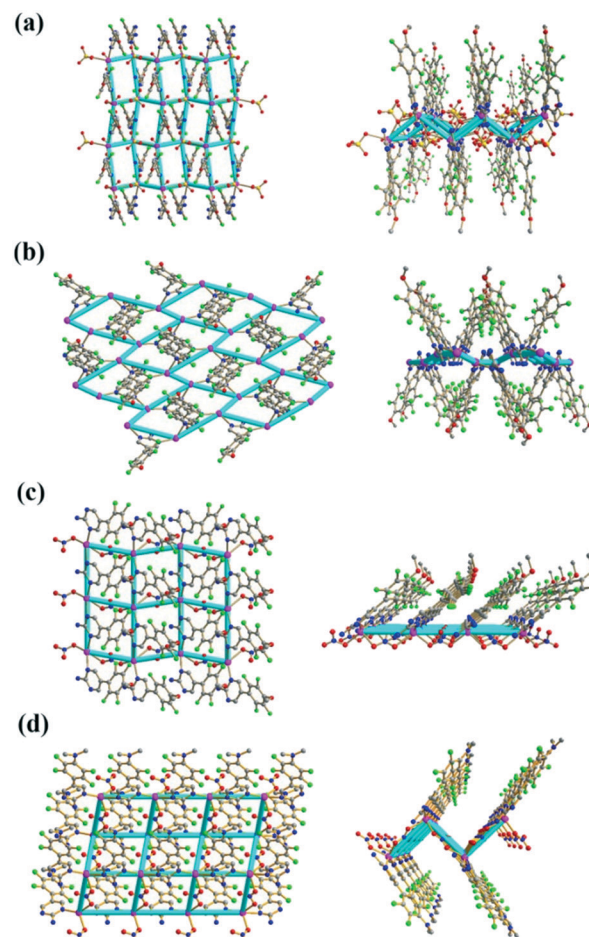


**Fig. 8** The 2D layer for **76–79** (a-d) viewed from different directions. (Purple ball: Ag; blue ball: N; gray ball: C; green ball: F; red ball: O).

$[\text{AgN}_2\text{O}]$  and  $[\text{AgNO}_2]$  trigonal geometries. The shortest  $\text{Ag}\cdots\text{Ag}$  distance is 3.573(1) Å which is longer than twice the van der Waals radii of silver. The  $\text{NH}_2\text{dmpym}$  and nipa ligands act as bidentate angular donor and  $\mu_4\text{-O}$ -donor, respectively, to link  $\text{Ag}(\text{i})$  ions to a 2D double layer along the *bc* plane (Fig. 9) in which the  $\text{NH}_2\text{dmpym}$  and nipa ligands alternately stack to a column along the *b* axis through the  $\pi\cdots\pi$  interactions with centroid-to-centroid distances of 3.584(3) and 3.585(3) Å.<sup>54</sup> It's worthy to note that abundant noncovalent interactions, such as  $\text{lp}(\text{O}_{\text{carboxyl}})\cdots\pi$ ,  $\pi\cdots\pi$ ,  $\text{C}-\text{H}\cdots\pi$  interactions and hydrogen-bonding, contribute largely

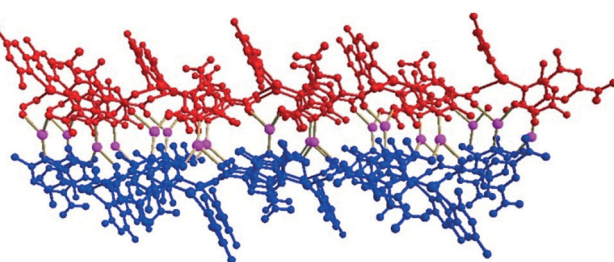


**Fig. 9** The 2D bilayer structure of **80**.

to generate a 3D supramolecular framework in the final product.

Complex 85, a mixed-ligand pillared bilayer, was reported by our group.<sup>41</sup> X-ray single-crystal analysis reveals that it crystallizes in the orthorhombic acentric space group *Pca2*<sub>1</sub>. In 85, one Ag(i) adopts a [AgN<sub>2</sub>O<sub>3</sub>] distorted square pyramidal geometry with a  $\tau_5$  factor of 0.16 (the  $\tau_5$  value for an ideal square pyramid is 0),<sup>64</sup> and the other two are in distorted tetrahedral geometries ( $\tau_4 = 0.78$  and 0.81).<sup>65</sup> The mal anion shows bidentate chelation through O<sub>2</sub> and O<sub>4</sub> towards Ag1 to form a six-membered ring with twist-boat conformation indicated by RPA (Ring Puckering Analysis) [ $\theta = 86.9(7)$ °,  $\phi = 275.8(6)$ °]<sup>66</sup> and  $\mu_2$ -bridging coordination modes. There is no evidence of any Ag(i)···Ag(i) interactions, the closest Ag···Ag distance is 3.56 Å between the two adjacent Ag(i) ions. In a whole view, the NH<sub>2</sub>pym ligands in a bidentate fashion link the Ag(i) ions to form zig-zag chains which are further extended to a 2D irregular 4<sup>4</sup>-sql single sheet by a  $\mu_2$ -O bridge of mal ligands along the *ac* plane (Fig. 10a). The single layer was further interlinked to form a 2D double sheet structure through pillared mal ligands (Fig. 10b). The amino group and acceptor O atoms from mal ligands form two different hydrogen bond motifs: R<sub>4</sub><sup>3</sup>(10) and R<sub>4</sub><sup>3</sup>(12).<sup>67</sup>

The firstly unmasked interpenetrated structure in the 2D family is 87 (Fig. 11). Normally, short ligands disfavor the entangled structure, however, the oligomeric [Ag-NH<sub>2</sub>pym]<sub>2</sub> subunit acting as a long ligand and an undulated feature facilitates the formation of an interpenetrated structure. The structure of 87 shows an argentophilic interaction consolidated 2-crossing [2]-catenane motif formed between pairs of parallel interpenetrating 2D 4<sup>4</sup>-sql nets. Complex 87 crystallizes in the monoclinic space group *C2/c*. Analysis of the local symmetry of the metal atoms and ligands showed that both Ag(i) atoms reside on the crystallographic *C2* axis; the suc and water molecules are located on the inversion centers. Two unique Ag(i) atoms are located in distorted tetrahedral ( $\tau_4 = 0.76$ ) and linear geometries (bond angle of N-Ag-N = 160.6(3)°). In 87, the Ag(i) ions are linked by bidentate NH<sub>2</sub>dmpym and suc ligands to form a single 2D undulated net (Fig. 11a). In each net, the window comprising Ag<sub>4</sub>(NH<sub>2</sub>dmpym)<sub>4</sub>(suc)<sub>2</sub> has a size of 12.36 × 9.17 Å<sup>2</sup> based on the Ag···Ag distances, which is large enough to allow the metal-organic rod from another window to penetrate. In 87, tetrahedral Ag1 and linear Ag2 are in 4- and 2-connected

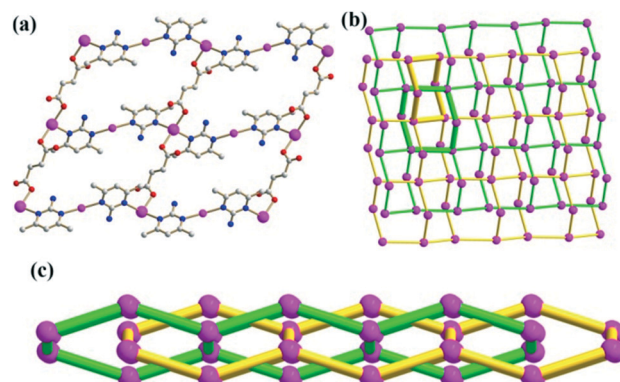


Fig. 11 (a) A view of the undulated 4<sup>4</sup>-sql net in the structure of 87. Ag2 ions as 4-connected nodes are shown in bigger balls. (Purple ball: Ag; blue ball: N; gray ball: C; red ball: O). (b) Schematic representation of the interpenetration of a pair of undulated 4<sup>4</sup>-sql nets in 87. The 2-crossing [2]-catenane motif is highlighted in yellow and green. (c) Side view of the interpenetration of a pair of undulated 4<sup>4</sup>-sql nets 87.

nodes, respectively, which are linked by 2-connected NH<sub>2</sub>dmpym and suc ligands. So the 2D net can be simplified to a 4<sup>4</sup>-sql net,<sup>68</sup> which is not a single net but shows the interesting 2D + 2D → 2D parallel interpenetration (Fig. 11b). Because the interpenetrated nets are parallel to each other and are coincident, thus the overall dimensionality increase does not happen (Fig. 11c). Different from the previous documented 2D + 2D → 2D parallel interpenetrating coordination compounds,<sup>69</sup> the pairs of 4<sup>4</sup>-sql nets in 87 are further supported by argentophilic interactions (3.2770(16) Å) which lock up the potential slippage of two entangled nets. Alternatively, if Ag···Ag interactions in 86 are included in simplification, the entanglement should be interpenetrated + interlocked, that is, self-penetration.<sup>70</sup>

Our group reported a series of Ag(i) coordination compounds (92–95) derived from aminopyrimidyl ligands and dicarboxylates which are 4<sup>4</sup>-sql nets with different sizes and shapes of rectangle windows. When NH<sub>2</sub>pym and suc were used as linkers, the structure of 92 is very similar to that of 87 and belongs to the 2D + 2D → 2D parallel interpenetration network based on the wavy 4<sup>4</sup>-sql single layer incorporating a window of 9.33 × 12.22 Å<sup>2</sup> based on the Ag1···Ag1 distances (Fig. 12). Two single layers shift with respect to another one with a slippage of *ca.* 6.11 Å. The residue void after interpenetration was occupied by lattice water molecules which are hydrogen-bonded to carboxylic groups with an O<sub>water</sub>–H···O<sub>suc</sub> distance of 2.761(3) Å, moreover, amino groups of NH<sub>2</sub>pym also interact with the carboxylic groups through N–H···O<sub>suc</sub> hydrogen bonds with an average distance of 2.853(4) Å, both of them reinforce the resultant interpenetrated 2D nets.

Compounds 93–95 are non-interpenetrated 4<sup>4</sup>-sql sheets (Fig. 13). When NH<sub>2</sub>pym and glu were used as 2-connected linkers, the Ag(i) ions in 93 are linked by NH<sub>2</sub>pym to form 1D single zigzag chains in which the NH<sub>2</sub>pym is oppositely arranged. A pair of adjacent chains was bound together to each other by Ag···Ag interaction (Ag1···Ag2 = 3.1284(7) Å) to

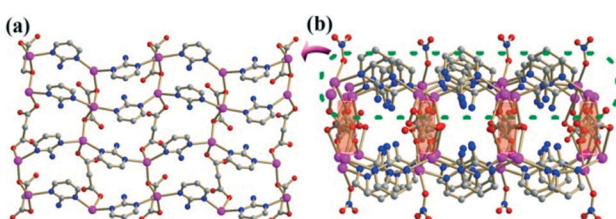


Fig. 10 (a) The 2D irregular 4<sup>4</sup>-sql single sheet in 85. (b) The 2D pillared-bilayer structure of 85. (Purple ball: Ag; blue ball: N; gray ball: C; red ball: O).

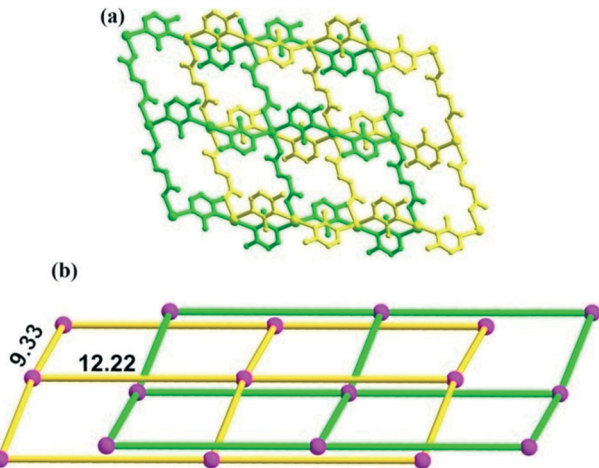


Fig. 12 (a) Ball-and-stick representation of the interpenetration of a pair of undulated 2D sheets in 92. (b) Interpenetrated two simplified 4<sup>4</sup>-sql nets (networks individually colored).

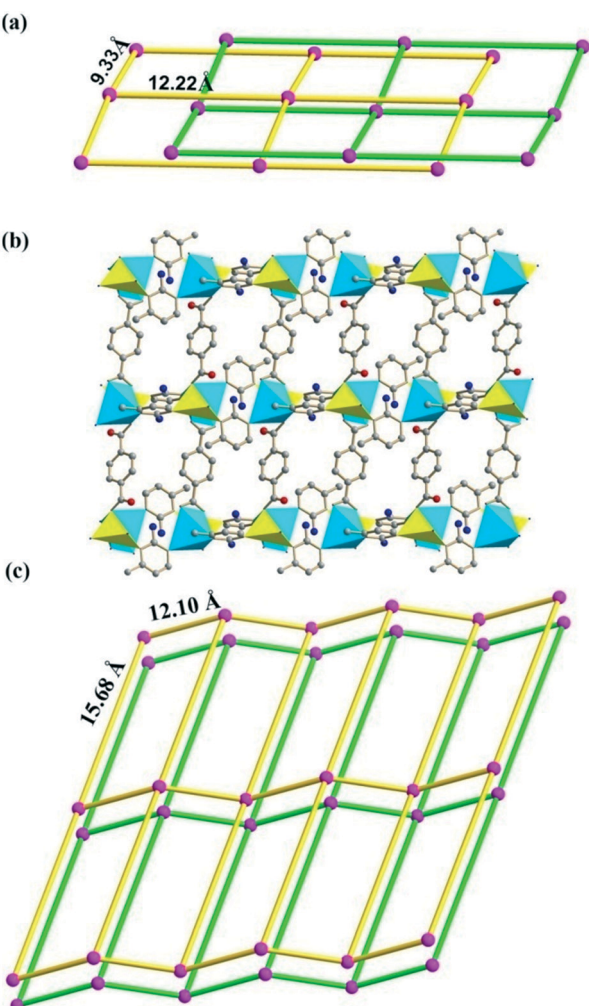


Fig. 13 Schematic representation of the 4<sup>4</sup>-sql nets of 93 (a), 94 (b), and 95 (c).

form a double-chain. The curled glu ligands extend the 1D double chains into a 2D double-sheet incorporating a window

of  $12.46 \times 10.04 \text{ \AA}^2$ , which is clearly larger than that in 92, but no interpenetration was found due to the less undulation degree of the 2D sheet in 93. When aromatic dicarboxylate was introduced into this system, we observed 94 as a double-layer. Different from 93, there is no any Ag···Ag interaction between adjacent 1D single chains in 94. The Ag(I) atom is bridged by  $\mu_2\text{-}\eta^2\text{:}\eta^0$  carboxylic groups of tpa into the resultant 1D double chain. Notably, the tpa ligands demonstrate  $\mu_2\text{-}\eta^1\text{:}\eta^1\text{:}\eta^1\text{:}\eta^1$  chelating and  $\mu_4\text{-}\eta^2\text{:}\eta^0\text{:}\eta^2\text{:}\eta^0$  bridging modes, which arrange alternately along the 1D double chains and extend them into a 2D net. Using longer bbdc in this family, X-ray analysis reveals that 95 crystallizes in a monoclinic system with space group *C*2/c. Two Ag(I) ions are located in distorted tetrahedral and linear geometries, excluding the Ag···Ag interaction. The Ag(I)-NH<sub>2</sub>dmpym 1D single zigzag chains interact with the adjacent chain to form a double-chain *via* Ag···Ag interaction of 3.1284(7) Å. The  $\mu_2\text{-}\eta^1\text{:}\eta^0\text{:}\eta^1\text{:}\eta^0$  bbdc ligands with a dihedral angle between two phenyl rings of 40.2(3)° extend the 1D chains into a double 4<sup>4</sup>-sql net incorporating a window of  $12.10 \times 15.68 \text{ \AA}^2$ .

Compounds 83 and 84 are built from Ag(I) ions and H<sub>2</sub>tcpta with NH<sub>2</sub>pym or NH<sub>2</sub>dmpym.<sup>57</sup> Single-crystal X-ray diffraction analysis has revealed that both of them are 2D layers. In 83, the Ag(I) ions are linked by bidentate NH<sub>2</sub>pym ligands to form zigzag chains, which are connected by the  $\mu_2$ -tcpta ligands into 2D sheets. The NH<sub>2</sub>pym and tcpta ligands alternately arrange along the *a* axis and are stacked through  $\pi\cdots\pi$  interactions with centroid···centroid distances in the range of 3.3788(16)–3.6008(15) Å. In 84, the Ag-tepta 1D chains were linked by  $\mu_2$ -NH<sub>2</sub>dmpym ligands, producing a 2D sheet. The arrangement of NH<sub>2</sub>dmpym and tepta is alternating along the *c* axis incorporating weak  $\pi\cdots\pi$  interactions (centroid···centroid = 3.644(3) Å). In the packing of 2D layers of 83 and 84, there are abundant Cl···Cl and Cl···O halogen bonds to consolidate the resultant 3D supramolecular frameworks. Topologically, the single metal centers in 83 and 84 are 3- and 6-connected node, respectively. The resultant topologies are 3-connected fes (point symbol: {4·8<sup>2</sup>}) and 6-connected SP 2-periodic net (6,3)III (point symbol: {3<sup>6</sup>·4<sup>6</sup>·5<sup>3</sup>}) for 83 and 84, respectively (Fig. 14).

Chen's group used different anions to construct compounds 96–98 as a series of 2D structures based on Ag(I) ions with NH<sub>2</sub>pym or NH<sub>2</sub>dmpym. The crystals of 96 crystallized in the chiral space group *P*2<sub>1</sub>2<sub>1</sub>2 (Flack parameter: -0.03(6)). The Ag(I) ion is coordinated by three N atoms of three NH<sub>2</sub>pym rings, giving a distorted triangular planar geometry (the sum of the three N-Ag-N angles: 359.9°), so the Ag(I) ion is a 3-connected node, which is linked by bidentate NH<sub>2</sub>pym ligands to form an undulated 6<sup>3</sup>-hcb molecular network. The ClO<sub>4</sub><sup>-</sup> anions interact with adjacent sheets through C-H···O and N-H···O hydrogen bonds (Fig. 15a).

When CH<sub>3</sub>COO<sup>-</sup> is presented, compound 97 shows a Ag···Ag interaction extended 2D 4<sup>4</sup>-sql sheet. The Ag(I) ion is in a distorted triangular planar geometry [the sum of the three N-Ag-N/O angles: 359.1°]. The Ag(I) ions are extended by bidentate NH<sub>2</sub>pym to form a linear chain with sinusoid-

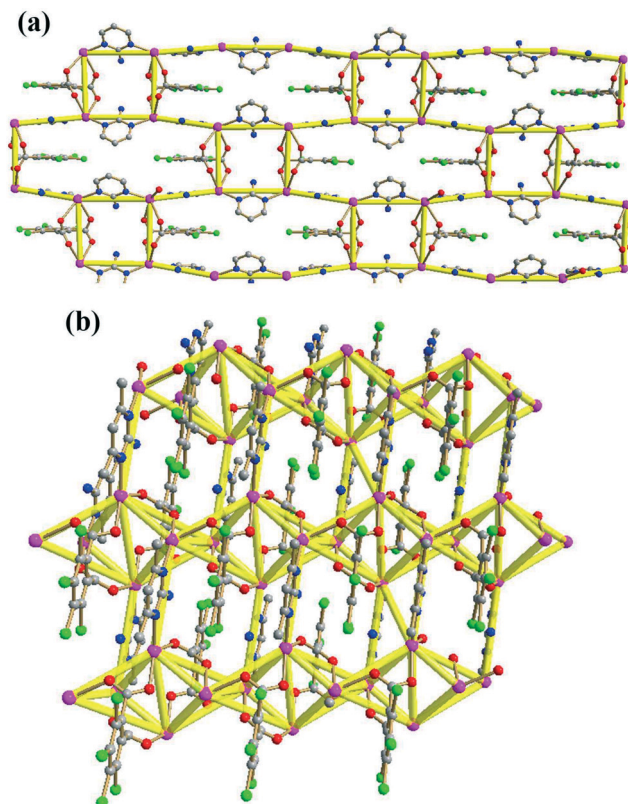


**Fig. 14** Schematic representation of 3-connected fes net and 6-connected SP 2-periodic net (6,3)III net for **83** (a) and **84** (b). (Purple ball: Ag; blue ball: N; gray ball: C; green ball: Cl; red ball: O).

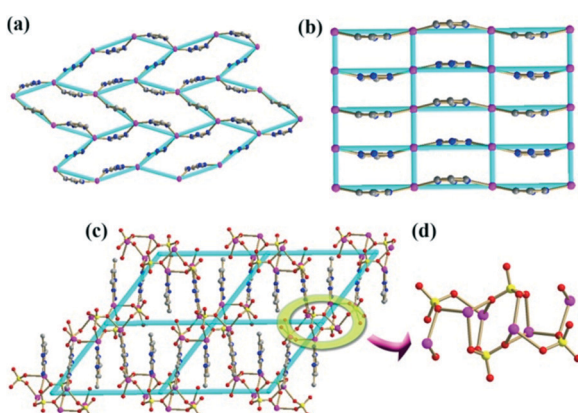


**Fig. 15** Schematic representation of 2D layered structures of **96** (a), **97** (b) and **98** (c). (d) The centrosymmetric  $[Ag_6(SO_4)_4]$  cluster. (Purple ball: Ag; blue ball: N; gray ball: C; yellow ball: S; red ball: O).

like conformation, which are further extended by Ag···Ag interactions ( $Ag\cdots Ag = 3.15 \text{ \AA}$ ) to form a 2D wavy 4<sup>4</sup>-sql net. The length and the width of the window in the network are 6.35 and 3.15  $\text{\AA}$ , respectively (Fig. 15b).

Compound 98 is a rare  $[Ag_6(SO_4)_4]$  cluster based coordination network. There are four kinds of Ag(i) ions, Ag1–Ag3 participated in the formation of the  $[Ag_6(SO_4)_4]$  cluster, which could be seen as a centrosymmetric  $Ag_4$  rectangle adding two

additional Ag atoms up and down the rectangular plane with the help of the bridging  $SO_4^{2-}$  anions. Two binding modes of  $SO_4^{2-}$  anions,  $\mu_4\text{-O}:O':O''$  and  $\mu_3\text{-O}:O':O'$  were observed. The  $Ag_4$  rectangle has dimensions of  $3.66 \times 3.35 \text{ \AA}$ . The bidentate NH<sub>2</sub>dmpym linked the  $[Ag_6(SO_4)_4]$  cluster to the 2D undulated sheet. Taking this hexanuclear SBU as 4-connected node, this 2D net belongs to 4<sup>4</sup>-sql topology (Fig. 15c).

### 3.4. 3D network

No more than ten compounds are genuine 3D networks in this family. Compounds **102** and **103** show interesting 2D + 2D  $\rightarrow$  3D polycatenation. There are similar components in the structures of **102** and **103**, those are two crystallographically independent Ag(i) ions, two NH<sub>2</sub>dmpym or NH<sub>2</sub>mpym, one ipa dianion and two lattice water molecules in the asymmetric unit. In them, one Ag(i) ion is in a linear geometry and another in a distorted tetrahedron geometry. The  $\tau_4$  parameters are 0.73 and 0.77 for Ag2 in **102** and **103**, respectively. Similar to **87**, the basic structures of **102** and **103** are also a 4<sup>4</sup>-sql net which is constructed by Ag(i) ions, bidentate NH<sub>2</sub>dmpym or NH<sub>2</sub>mpym and ipa ligands. The 4<sup>4</sup>-sql net also contains one type of node (four-connected Ag2 ions) and two types of linkers (two-connected NH<sub>2</sub>dmpym or NH<sub>2</sub>mpym and ipa ligands). Compared to the net of **87**, the nets have larger windows of  $11.70 \times 11.51 \text{ \AA}^2$  and  $11.74 \times 11.43 \text{ \AA}^2$  and exhibit a highly undulated character with thicknesses of about 6.72 and 6.44  $\text{\AA}$  in **102** and **103**, respectively. As a result, each highly undulated 2D 4<sup>4</sup>-sql net is simultaneously penetrated by the two nearest neighbouring ones. In other words, each window is simultaneously catenated by the other two. Therefore, the 2D  $\rightarrow$  3D dimensionality enhancement should be ascribed to the polycatenation of the nets. Different from **87**, although the interpenetrating nets in **102** and **103** also have parallel mean planes, these mean planes are not concurrent but are offset, and thus an overall 3D entangled network is formed. The high degree of entanglement is due to: (i) the highly undulated characteristic of the single 4<sup>4</sup>-sql net; (ii) the enough large windows of the net; and (iii) the suitable packing orientation (Fig. 16).

Compound **104** is a pseudohalogen supported 3D framework. It crystallized in the orthorhombic space group *Pbcn*. The crystal structure of **104** consists of a AgSCN-NH<sub>2</sub>pym adduct in 2:1 stoichiometry. Each Ag(i) is in a distorted tetrahedral coordination geometry with bond angles opened up to  $133.68(8)^\circ$  from the ideal tetrahedral angle while the remaining angles are in the range from  $93.14(10)$  to  $114.60(8)^\circ$ . Each thiocyanate adopts  $\mu_3\text{-}\kappa^3S$  coordination mode to link three Ag(i) ions to form a  $Ag_3S_3$  boat-like six-membered ring and this repeated unit shares the Ag–S edges to extend the structure to a 2D honeycomb-like 6<sup>3</sup>-hcb net (Fig. 17a). It should be noted that **104** is the first compound showing a thiocyanate anion with  $\mu_3\text{-}\kappa^3S$  coordination mode and the characteristic infrared absorption band in spectra of  $\mu_3\text{-}\kappa^3S\text{-SCN}$  is in  $\sim 2130 \text{ cm}^{-1}$ . In **104**, coordination modes of thiocyanate correspond to Pearson's principle of hard and

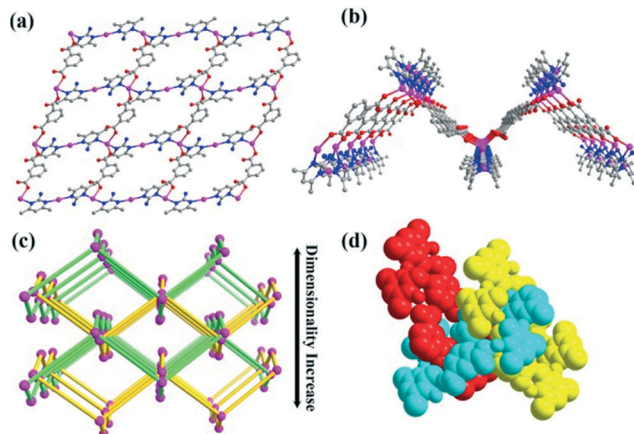


**Fig. 16** (a) and (b) View of the single undulated 4<sup>4</sup>-sql net in the structure of **102** along different directions. (Purple ball: Ag; blue ball: N; gray ball: C; red ball: O). (c) A view of the 2D + 2D → 3D polycatenation of the undulated 4<sup>4</sup>-sql nets in the structure of **102**. (d) A view of catenation of rectangular windows.

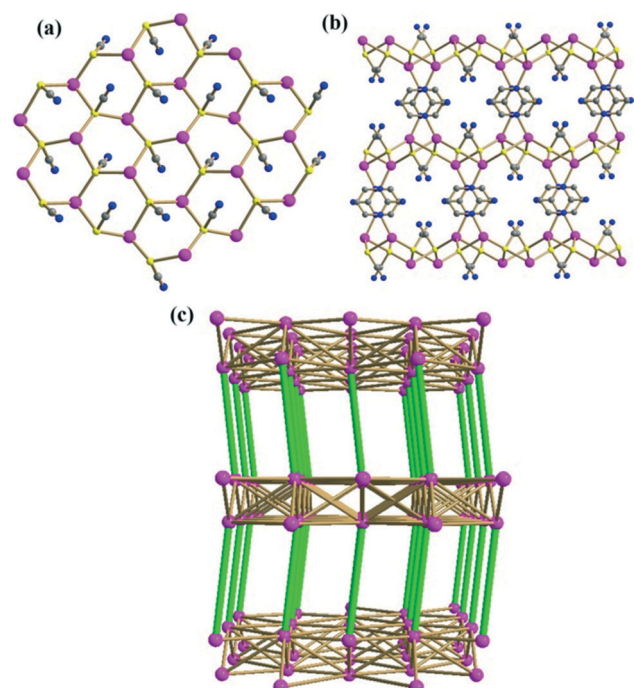


**Fig. 17** (a) Ball-and-stick representation of 2D 6<sup>3</sup>-hcb net. (b) View of the 3D NH<sub>2</sub>pym pillared framework. (c) Simplified 9-connected nce topology. (Green stick = NH<sub>2</sub>pym pillar; purple ball: Ag; blue ball: N; gray ball: C; yellow ball: S).

soft Lewis acids and bases (HSAB), according to which the “soft” Ag(i) ions should bind preferentially to the “softer” S atoms of the thiocyanate groups.<sup>72</sup> The adjacent 2D nets along the *bc* plane are further extended by μ<sub>2</sub>-N,N' NH<sub>2</sub>pym to the 3D framework (Fig. 17b). Based on TOPOS calculation<sup>73</sup> and taking the single Ag(i) ion as node, then this net could be simplified to a 9-connected nce topology with a Schläfli symbol of {3<sup>12</sup>.4<sup>18</sup>.5<sup>6</sup>} (Fig. 17c).

Compound **105** consists of a Ag<sub>2</sub>SO<sub>4</sub>-NH<sub>2</sub>pym adduct in 1:2 stoichiometry. The Ag(i) ion is coordinated by two pyrimidine nitrogen atoms, one amino nitrogen atom and one sulfate oxygen atom to form a distorted tetrahedral geometry. Each NH<sub>2</sub>pym ligand shows a rare μ<sub>3</sub>-N<sup>1</sup>:N<sup>1</sup>:N<sup>1</sup><sub>amino</sub> mode and is coordinated to three Ag(i) metal centers to form 2-D wavy molecular sheets (Fig. 18a), which then are interlinked by the SO<sub>4</sub><sup>2-</sup> anions to form a 3D framework (Fig. 18b). Taking each Ag(i) ion as node, each one is linked to six nearest others, so the resultant 3D network could be simplified to a vmd topology with a Schläfli symbol of {3<sup>3</sup>.4<sup>5</sup>.5<sup>6</sup>.6} (Fig. 18c).

Compound **106** is a mixed-ligand 3D coordination polymer with a high symmetry. The crystals of it conform to the space group *R*̄*3*. The charge neutrality is achieved by deprotonated carboxylate groups of the H<sub>3</sub>btc molecule. There is only a crystallographically unique Ag(i) center in the crystal structure. Each four-coordinated Ag(i), which adopts a distorted tetrahedral geometry, is coordinated by two bridging NH<sub>2</sub>pym nitrogen atoms, and two carboxylate oxygen atoms of two unique btc<sup>3-</sup> anions. Two centrosymmetric Ag centers in pairs were linked by two carboxylate groups from two unique btc<sup>3-</sup> anions, giving a dinuclear Ag<sub>2</sub>(COO)<sub>2</sub> SBU. Each NH<sub>2</sub>pym and btc<sup>3-</sup> connected to two and three SBUs, respectively, extending the SBU into a 3D network. From the viewpoint of topology, if the btc<sup>3-</sup> anions are considered as 3-connected nodes (extended point symbol is 4·4·4) and the Ag<sub>2</sub> SBUs are considered as 6-connected nodes (extended point symbol is 4·4·4·4·4·6<sub>2</sub>·6<sub>2</sub>·6<sub>2</sub>·6<sub>4</sub>·6<sub>4</sub>·8<sub>28</sub>·8<sub>28</sub>·8<sub>8</sub>), the whole 3D structure exhibits a rare binodal (3,6)-connected **loh1** topology with the vertex symbol {4<sup>3</sup>}<sub>2</sub>{4<sup>6</sup>·6<sup>6</sup>·8<sup>3</sup>}<sub>3</sub> calculated with TOPOS software (Fig. 19). As we know, the most frequent (3,6)-connected nets in MOFs are mainly focused on **rtl** net-(4·6<sup>2</sup>)<sub>2</sub>(4<sup>2</sup>·6<sup>10</sup>·8<sup>3</sup>), **pyr**-(6<sup>3</sup>)<sub>2</sub>(6<sup>12</sup>·8<sup>3</sup>), and **ant**-(4<sup>2</sup>·6)<sub>2</sub>(4<sup>4</sup>·6<sup>2</sup>·8<sup>8</sup>·10).<sup>74</sup> However, the limited (3,6)-connected **loh1**

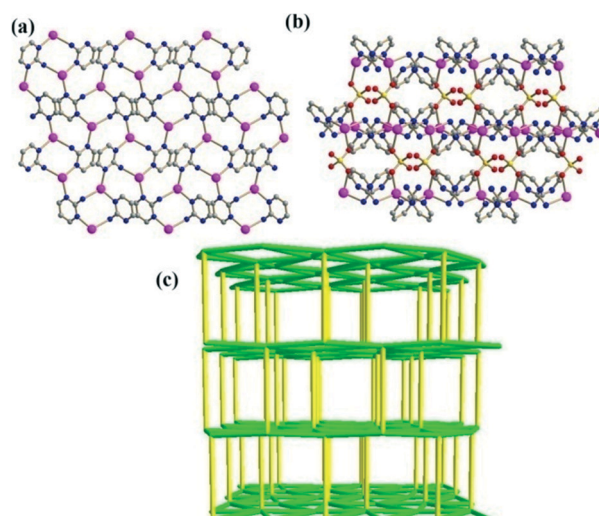


**Fig. 18** (a) Ball-and-stick representation of 2D net. (b) View of the 3D SO<sub>4</sub><sup>2-</sup> pillared framework. (c) Simplified vmd topology. (Yellow stick = SO<sub>4</sub><sup>2-</sup> pillar; purple ball: Ag; blue ball: N; gray ball: C; yellow ball: S).

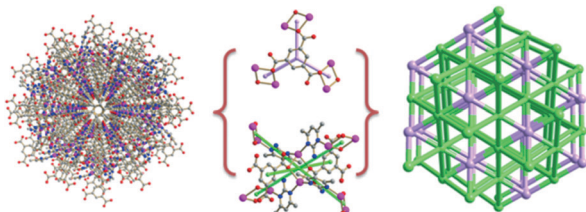


**Fig. 19** The 3D framework and its simplified topological network of **106**. (Purple ball: Ag; blue ball: N; gray ball: C; red ball: O).

frameworks for MOFs and inorganic materials have been documented so far.<sup>75</sup>

X-ray crystal structure determination displays that **107** consists of molecular bilayers with T-shaped blocks as the fundamental building units, in which each central Ag(I) cation adopts a Y-shaped coordination configuration. Each NH<sub>2</sub>pym as a bidentate ligand links Ag(I) centers to form infinite 1D chains. Fascinatingly, two kinds of extended modes are observed for these 1D chains. When viewed from above the *ab* plane, two related [Ag(NH<sub>2</sub>pym)]<sub>∞</sub> chains are interwoven. The deprotonated glu<sup>2-</sup> anions as pillars interlink the upper and lower chains to generate a bilayer motif. The width and height of the motif are determined by the length of the NH<sub>2</sub>pym ligand (6.45 Å) and glu anion (9.85 Å), respectively (Fig. 20).

Furthermore, a remarkable feature of the structure of **107** is that the bilayer is sustained by the long glu anion and short NH<sub>2</sub>pym ligand and displays an unusual tongue-and-groove structure. The parallel interpenetration of “thick” layers gives a new kind of 2D → 3D polycatenation: the 2-D layers interpenetrate each other in quintuple mode resulting in the 5-fold interpenetrating structure with Ag···Ag interactions (Fig. 21). The separations between silvers are alternatively 3.27 and 3.24 Å, which indicate the existence of weak Ag···Ag interactions. If the single metal center are taken as node, then the overall network could be simplified to a 6-connected osb/Cmcm-C2/c topology with vertex symbol {3<sup>3</sup>·4<sup>4</sup>·5<sup>7</sup>·6}.

When using rigid aromatic 14npd instead of glu to react with AgNO<sub>3</sub> and NH<sub>2</sub>pym, compound **108** with a different structural type from **106** was obtained. Single crystal X-ray analysis reveals that **108** crystallized in the orthorhombic space group *Pnna*. Two independent Ag(I) ions have similar

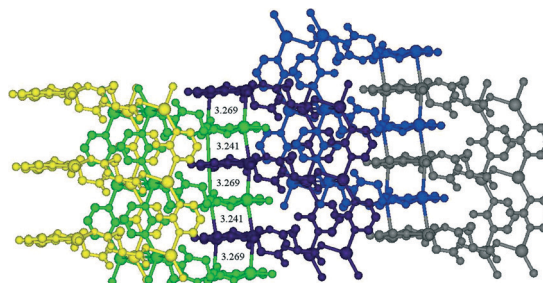


**Fig. 21** The 5-fold interpenetrating structure of **107** with Ag···Ag weak interactions.

tetrahedral coordination environments. Two centrosymmetric Ag centers in pairs were linked by two carboxylate groups to form a dinuclear Ag<sub>2</sub>(COO)<sub>2</sub> SBU, which is extended by two NH<sub>2</sub>pym and two 14npd to form the resultant 3D framework. Although SBU is the same in **106** and **108**, btc and 14npd have different connection numbers in constructing the 3D framework, thus Ag<sub>2</sub>(COO)<sub>2</sub> SBU in **108** is just linked to its nearest four neighbors, giving it a 4-connected dia network (Fig. 22).

The X-ray structural analysis reveals that **109** crystallized in the triclinic *P*̄*1* space group. The Ag1 and Ag2 adopt a slightly distorted T-shaped geometry, while Ag3 is coordinated to one O atom and two N atoms in a slightly distorted Y-shaped geometry. It is interesting to find that there were two kinds of Ag···Ag interactions in the structures of **109**: the first kind of Ag···Ag distances [Ag1···Ag1A = 2.786(2) and Ag2···Ag2B = 2.809(2) Å] is comparable to the Ag···Ag separation (2.89 Å) in metallic silver; the second kind of Ag···Ag distances [Ag1···Ag2A = 3.176(2) and Ag3···Ag3A = 3.253(3) Å] is shorter than the sum of van der Waals radii of Ag (*r*<sub>vdw</sub>(Ag) = 1.72 Å), which is suggestive of a weak interaction between the two metal silver centers. Each btc<sup>3-</sup> anion connects five Ag(I) atoms through three fully deprotonated carboxylates with μ<sub>2</sub>-η<sup>1</sup>:η<sup>1</sup>, μ<sub>2</sub>-η<sup>1</sup>:η<sup>1</sup>, and μ<sub>1</sub>-η<sup>2</sup> coordination modes. The μ<sub>2</sub>-N<sup>1</sup>:N<sup>1</sup> NH<sub>2</sub>pym ligand connects each pair of adjacent silver atoms via pyrimidyl nitrogen atoms to form 1D wavy pattern chains, which are further linked by btc<sup>3-</sup> anions to generate a 2D structure. Two types of cluster units aggregated by Ag···Ag

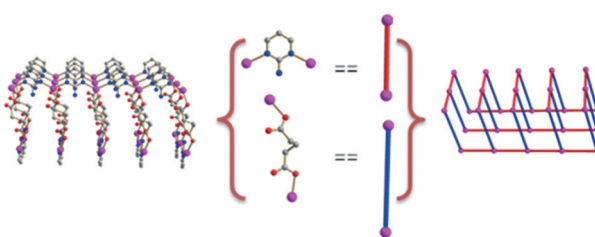


**Fig. 20** Schematic representation of molecular bilayer motif of **107**. (Purple ball: Ag; blue ball: N; gray ball: C; red ball: O).

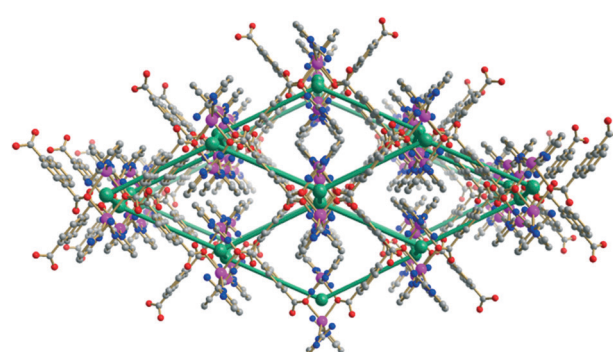


**Fig. 22** The 3D dia network of **108**.

interactions were observed, the carboxylate-supported  $\text{Ag}_3\cdots\text{Ag}_3$  dimer and the 1D carboxylate-supported infinite zigzag ( $\text{Ag}_1\cdots\text{Ag}_2\cdots\text{Ag}_2\cdots\text{Ag}_1)_n$  chain unit. Such rich  $\text{Ag}\cdots\text{Ag}$  interactions extend the  $\text{Ag}(\text{i})$  ions to a 1D chain running along the  $a$  axis supported by  $\mu_2$ -carboxylate bridges (Fig. 23a). These dimers and 1D  $\text{Ag}\cdots\text{Ag}$  chains are further linked by the  $\text{btc}^{3-}$  and  $\text{NH}_2\text{pym}$  ligands to form a 3D framework, in which the presence of ligand-unsupported  $\text{Ag}\cdots\text{Ag}$  interactions plays a vital role in the formation of the 3D coordination framework (Fig. 23b).

## 4. Influence of various factors on the assembly of $\text{NH}_2\text{pym}$ and its derivative based silver(**i**) coordination architectures

$\text{NH}_2\text{pym}$  and its derivatives were demonstrated to construct a variety of networks ranging from 0D, 1D, 2D to 3D with several silver(**i**) salts in the presence or absence of a secondary ligand. The diversity of the coordination architectures was shown to depend on several factors such as anion, substituent, solvent, and auxiliary ligand. In the following sub-sections, we will illustrate these factors by exemplifying based on discussed structures above.

### 4.1. Influence of anion effect

In metal-ligand-assembled architectures, the dominant factor that controls the final structure is usually the metal-ligand coordination interaction, and any structure formed at last

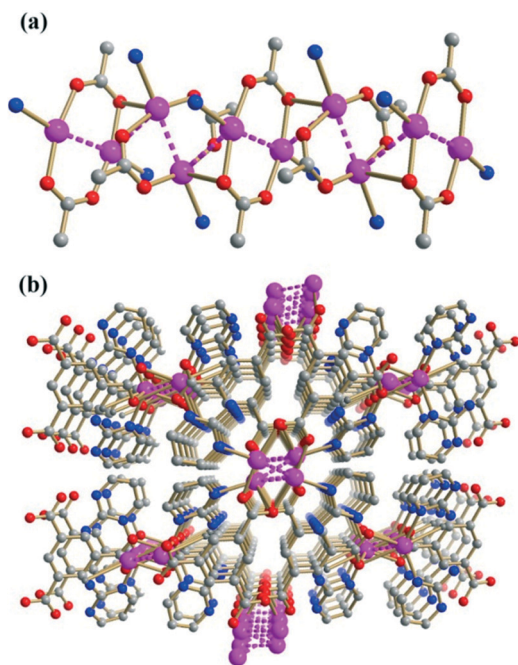


Fig. 23 (a) The silver chain along the  $a$  axis, (b) perspective view of the 3D network along the  $a$  axis direction in 109.

must fulfill the requirements of the metal ion. The  $d^{10}$   $\text{Ag}(\text{i})$  ion lacks preferred coordination geometries, so weak noncovalent interactions from the anion may also have a strong effect and determine the organization of the coordination structures.<sup>76</sup> It has long been known that anions of different size and coordination ability play important roles in the assembly of different structures through involving in the coordination with the metal center.<sup>77</sup> Recent studies also disclosed that the anions chosen for their “relative innocence” in terms of coordinating ability can nevertheless manipulate the assembly process *via* noncovalent interactions such as hydrogen bonding, anion $\cdots\pi$  and van der Waals forces.<sup>78</sup>

Chen's group reported that the assembly of different silver salts ( $\text{AgNO}_3$  and  $\text{AgCF}_3\text{SO}_3$ ) with I-apym under the same conditions could afford two series of anion-controlled 0D metal-organic macrocycles and 1D helical chains (Fig. 24). For 14 and 17, they are 16-membered  $\text{Ag}_4(\text{I-apym})_4$  and 24-membered  $\text{Ag}_6(\text{I-apym})_6$  macrocycles, respectively, which should be controlled by the anion sizes, that is, a larger anion preferred a larger macrocycle motif.<sup>7,23</sup> In the presence of  $\text{PF}_6^-$  and  $\text{ClO}_4^-$ , assembly of  $\text{Ag}(\text{i})$  and I-apym gives two 1D helical chains of 56 and 57.<sup>7</sup> The helical chains in them run along  $4_1$  and  $2_1$  axes, and the helical pitches are 22.584 and 11.456 Å, respectively. The formation of different 1D helical chains is related to anion effects including their coordination ability and the formed hydrogen bonding with chains. It is clearly seen that in 56 the  $\text{PF}_6^-$  anions are not included in the channel but outside the channel and weakly interact with the  $\text{Ag}(\text{i})$  through  $\text{Ag}\cdots\text{F}$  interactions as well as  $\text{N}-\text{H}\cdots\text{F}$  and

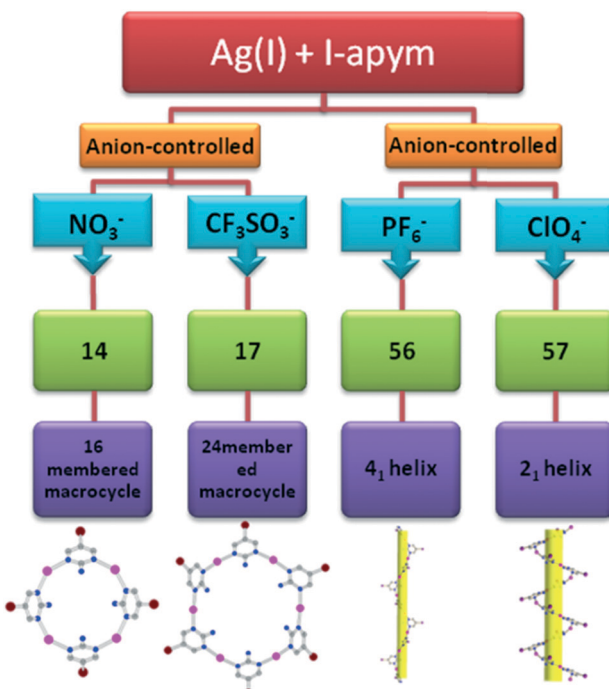


Fig. 24 Schematic representation of anion-dependent isolation of different macrocycle and 1D helical structures.

C–H···F hydrogen bonds. However, the channel in the helical chain of 57 is large enough to include the  $\text{ClO}_4^-$  anion, which links the Ag(I) through abundant Ag···O, N–H···O and C–H···O interactions. Thus, the Ag··· $\text{ClO}_4^-$ ···Ag interactions, linear  $\cdots(\text{Ag}\cdots\text{I}\cdots\text{Ag})_n\cdots$  interactions and hydrogen bonds in 57 diminish the length of the helical pitch of the helical chain. If I-apym was changed to Cl-apym, a zigzag chain 34 and a similar helical chain 63 were obtained under the direction of  $\text{CF}_3\text{SO}_3^-$  and  $\text{ClO}_4^-$  anions.<sup>23</sup>

Mattay and Eberhard's group reacted nfapym with different silver salts, giving four 1D chain structures (26–29) and one 2D sql network (79).<sup>40</sup> When smaller  $\text{NO}_3^-$  and  $\text{ClO}_4^-$  were used, they obtained 26 and 29 as double-strands but larger  $\text{CF}_3\text{SO}_3^-$  and  $\text{CF}_3\text{CO}_2^-$  caused single zigzag chains in 27 and 28. It should be noted that 29 and 79 are a pair of genius supramolecular isomers<sup>79</sup> because they have the completely same components but different structure motifs (Fig. 25). The structural differences are mainly caused by  $\mu_2\text{-O:O}$  and  $\mu_2\text{-O:O}'\text{NO}_3^-$  anions. The former kind of  $\text{NO}_3^-$  anions binds two single chains to a double-strand, whereas the latter one binds adjacent single chains one by one to form a 2D sql net. It is difficult to discuss the origination of this supramolecular isomerism due to too much variables with regard to the synthetic conditions. The different amount of reactants, solvent volume, and reaction time as well as filtration or not may be the culprit.

Our group also found a series of coordination structures that ranges from 0D binuclear compound (18), 1D ladder (69), to 1D linear chain (70) depending on  $\text{ClO}_4^-$ ,  $\text{CF}_3\text{CO}_2^-$ , and  $\text{CF}_3\text{SO}_3^-$ , respectively (Fig. 26).<sup>32</sup> The  $\text{ClO}_4^-$  does not coordinate to the Ag(I) ion but weakly interact with it and form hydrogen bonding with  $\text{NH}_2\text{dmpym}$ , so it naturally is a guest anion and does not extend the binuclear unit to higher dimensionalities. The  $\text{CF}_3\text{CO}_2^-$  anion adopts a  $\mu_2\text{-O:O}'$  mode to link the  $[\text{Ag-NH}_2\text{dmpym}]_n$  single chain to the 1D ladder, where  $\text{CF}_3\text{SO}_3^-$  is in a  $\mu_1\text{-O}$  fashion, so it just acts as a terminal ligand to dangle on the  $[\text{Ag-NH}_2\text{dmpym}]_n$  single chain,

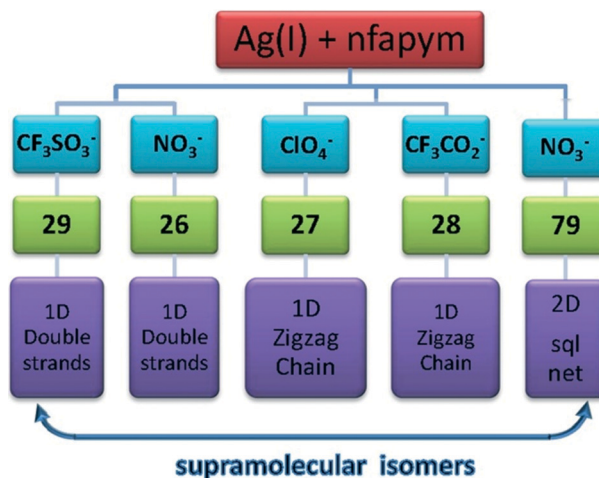


Fig. 25 Schematic representation of anion-dependent isolation of various 1D structures and a 2D net.

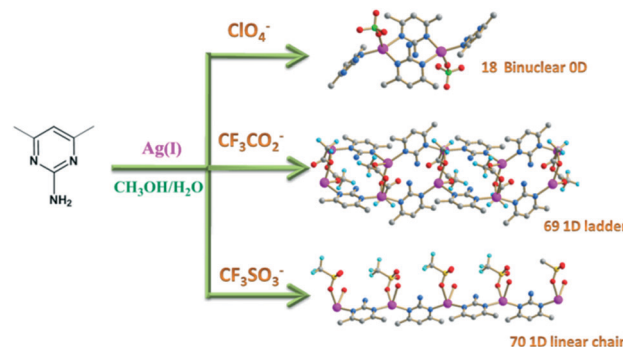


Fig. 26 Schematic representation of anion-dependent 0D and 1D structures.

forming a zigzag chain. The coordination abilities of three anions have the following order,  $\text{ClO}_4^- < \text{CF}_3\text{SO}_3^- < \text{CF}_3\text{CO}_2^-$ , which is responsible for the formation of the different structure motifs.

Hu's group designed a pyridyl-modified  $\text{NH}_2\text{pym}$  and used it to assemble with different silver salts, and got one 0D molecule (21) and two 1D chains (42 and 43).<sup>35</sup> The  $\text{NO}_3^-$  and  $\text{CF}_3\text{SO}_3^-$  ions yield 0D centrosymmetric binuclear 21 and 1D 42, respectively (Fig. 27). When counteranions  $\text{SCN}^-$  were used and coordinated with the metal ions, the 1D ladder 43 was isolated. In three compounds, the dpyapym-2 ligand uniformly adopts a bis-chelating coordination mode to bind with two silver atoms, but three distinct structural motifs were formed due to the different arrangements of the dpyapym-2 ligands in the three compounds. Thus, it is reasonable that the counteranions exerted a tuning effect on the formation of crystal structures.

#### 4.2. Influence of substituent group

The network structures of coordination compounds are usually influenced by the substituents attached to the backbones of organic ligands in the following two ways: (i) additional interconnecting functions to extend the coordination motifs by their coordination and secondary interactions; (ii) the substituents such as methyl and ethyl may impose significant

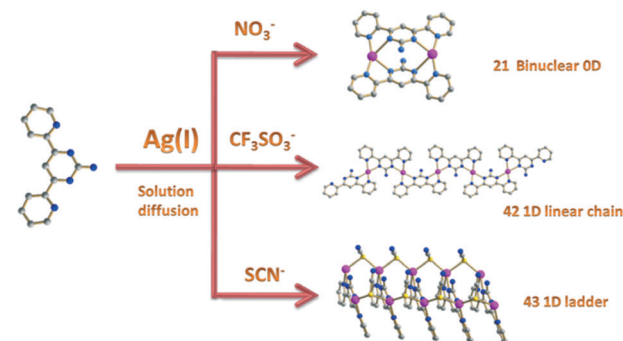


Fig. 27 Schematic representation of anion-dependent 0D and 1D structures of 21, 42 and 43.

steric and/or electronic effects on the coordination preferences of parent ligands, and consequently, the network structures of the resulting coordination compounds.

The current summarized compounds have presented that substituent groups on parent 2-aminopyrimidine possess negligible binding abilities with center metal ions and have often been employed as strategy (ii) to modulate the structures. In this highlight, parent 2-aminopyrimidine has been found to be modified at its 4-, 5-, and 6-position by Me, MeO, X (X = Cl, Br, I), pyridyl, aryl, and fluoroarene groups. Generally speaking, larger and more substituents may have a great tendency to generate lower dimensional structures due to their steric hindrance. In the first glance, all 3D frameworks are built from NH<sub>2</sub>pym or Me-substituted NH<sub>2</sub>pym, whereas larger groups such as pyridyl, aryl, and fluoroarene substituted NH<sub>2</sub>pym usually gave 0D, 1D or 2D motifs.

In several families of Ag(i)-aminopyrimidyl-carboxylate coordination compounds, the above-mentioned general regularity is well justified. With the number of substituted methyl groups increasing from 0 to 2, we obtained 41, 86 and 101 assembled from Ag(i), aminopyrimidyl and nitrilotriacetic acid as 1D zigzag chain, 2D 10<sup>3</sup> network, and 3D framework (Fig. 28), in which NH<sub>2</sub>pym and NH<sub>2</sub>mpym show μ<sub>2</sub>-N<sup>1</sup>:N<sup>1</sup> mode but NH<sub>2</sub>dmpym just acts as a monodentate ligand, so different dimensionalities of structures were generated.<sup>44</sup> Similarly, in two Ag(i)-aminopyrimidyl-malonate compounds, NH<sub>2</sub>pym produces a 2D pillared bilayer structure of 85, whereas NH<sub>2</sub>dmpym just induces formation of a 1D zigzag chain of 31.<sup>41</sup> When dicarboxylate and tricarboxylate were replaced with tetracarboxylate, we still observed similar regularity. Compound 46 is a 1D chain with NH<sub>2</sub>dmpym as a monodentate ligand, whereas 88 is a 4<sup>4</sup>-sql net with NH<sub>2</sub>pym as a bidentate bridge.<sup>47</sup> As we know, the methyl group is an electron-donating group, which should enhance the coordination ability of NH<sub>2</sub>mpym or NH<sub>2</sub>dmpym, compared to NH<sub>2</sub>pym. However, NH<sub>2</sub>mpym or NH<sub>2</sub>dmpym usually acts as a monodentate ligand, which demonstrated that the steric hindrance not the electronic effect of the methyl group predominates the assembly process.

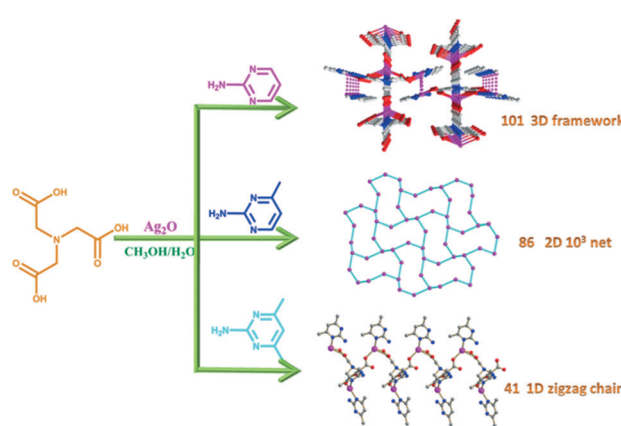


Fig. 28 Schematic representation of influence of substituent group on assembly of 1D–3D structures.

For 57, 63 and 64, they are assembled from AgClO<sub>4</sub> and X-apym (X = Cl, 63; Br, 64; I, 57) under similar conditions and show similar helical chains but with different repeated unit lengths, which may arise from different supramolecular interactions related to halogen bonding or hydrogen bonding (Fig. 29).<sup>7,23</sup> When assembling AgClO<sub>4</sub> with NH<sub>2</sub>dmpym, NH<sub>2</sub>mpmpy, and dmoapym, compounds 18, 72 and 75 were obtained as binuclear 0D molecule, 1D double-strand and 2D undulated sql network. The formation of diverse structural motifs is also influenced by the differences between methyl and methoxy groups.<sup>32</sup>

#### 4.3. Influence of solvent

The influence of the solvent system on assembly of metal-organic coordination compounds has recently been reviewed by Du's group.<sup>80</sup> The solvent effects influence assembly usually in the following four ways: (i) solvent as ligand in the host structure; (ii) solvent as guest in the crystal lattice; (iii) solvent as both ligand and guest; (iv) structure-inducing molecule in the absence of final products. Given to the former three ways, the solvent as reactants was incorporated on the host to influence the resultant structure. In the fourth case, no solvent could be found in the product but indeed subtly affects the crystal growth, crystal morphology, and overall connectivity of the final solid. In this case, the role of solvent in regulating the coordination systems cannot be definitely ascribed to an individual reason, so the synergy effect of several factors may be the best reason to explain how solvent impacts the assembly processes.

Compounds 53 and 73 are a pair of solvent-dependent products when AgNO<sub>3</sub> and dmoap are reacted in water-MeOH (v/v = 1 : 1, 10 mL) and water-EtOH (v/v = 1 : 1, 10 mL), respectively.<sup>28</sup> Two compounds have the same formulae but different 1D chain motifs, single zigzag chain and triple-strand, respectively. Solvent molecules are neither incorporated in the host nor lattice of the crystal (Fig. 30). In nature,

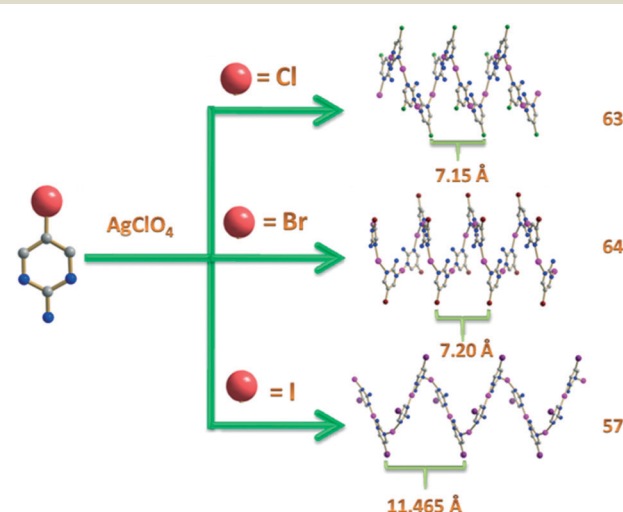
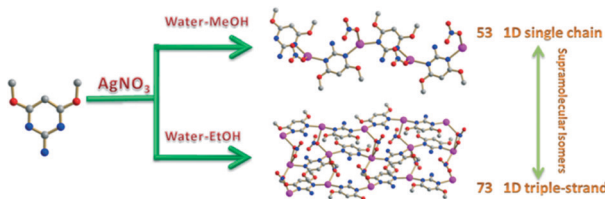


Fig. 29 Schematic representation of influence of halogen atom on assembly of 1D helical chains.



**Fig. 30** Schematic representation of solvent-controlled 1D single chain and triple-strand chain.

they are also a pair of genuine solvent-controlled supramolecular isomers.

Mattay's group also found that crystallization of  $\text{AgCF}_3\text{SO}_3$  and fapym in EtOH and  $^i\text{PrOH}$  will give compounds **60** and **61**, which have been found by the incorporation of respective solvent molecules in the host 1D chain.<sup>50</sup> The coordination chains of **60** and **61** are aligned vertically in crystal packing, and their geometric parameters are similar. The main dissimilarity between them is that single strands of **60** are aligned parallel to each other but are displaced by a half repetition unit along the *b*-axis whereas single strands of **61** are aligned without structural displacement along the *b*-axis. Interestingly, **60** and **61** can be transformed into the unsolvated intermediate  $[\text{Ag}(\text{fapym})(\text{SO}_3\text{CF}_3)]_n$  by heating at 120 °C for different times, which then could reversibly return to the original phase by subsequent addition of the respective solvent. The diffractogram from powder X-ray diffraction also proved that the reversible phase transitions of a polycrystalline sample of **60** into **61** is *via* an unsolvated intermediate  $[\text{Ag}(\text{fapym})(\text{SO}_3\text{CF}_3)]_n$  (Fig. 31). Moreover, crystals of **60** can be immersed in water or 2-propanol without heating, and a phase transition occurs immediately in water but overnight in 2-propanol. Differential scanning calorimetry (DSC) indicated that a phase transition under solvent extrusion is found at 108 °C and 105 °C for **60** and **61**, respectively.

#### 4.4. Influence of auxiliary ligand

The mixed-ligand assembly strategy facilitates the self-modulation of reaction parameters, such as alkalinity or acidity and solubility of the assembled system. While in the microscopic level, the free spaces around metal ions can be easily occupied by coordination with the mixed ligands,

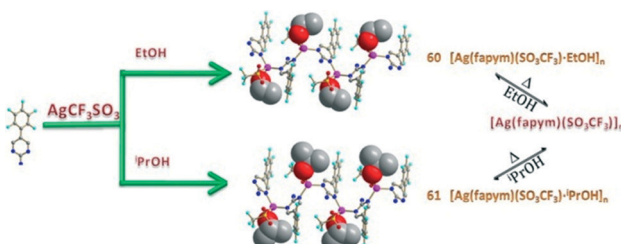


**Fig. 31** Schematic representation of solvent-controlled 1D zigzag chain and reversible transformation between different phases.

instead of solvents or anions; this may improve the stability of the resulting coordination architectures and increase the connectivity of the network, producing high dimensional networks. It has been reported that changing the auxiliary ligand in one reaction system can produce various coordination compounds with different dimensions and/or symmetries under certain circumstances.<sup>80</sup> The influence of the auxiliary ligand is mainly from linker length and geometry, coordination mode and ligand conformation. In this highlight, the secondary ligand is mainly carboxylates, which participated into the Ag-aminopyrimidyl system, producing diverse structures. The aminopyrimidyl and carboxylates belonging to the acid–base system are perfect collaborators that can compensate for charge balance without small anion, coordination unsaturation, and supramolecular interactions all at once.

In the  $\text{Ag}/\text{NH}_2\text{pym}/\text{carboxylate}$  family, totally 14 compounds were summarized based on varied carboxylates ranging from monocarboxylate, dicarboxylate, tricarboxylate to tetracarboxylate, and from aliphatic polycarboxylate to aromatic polycarboxylate. For monocarboxylates, when using bnb and bza as auxiliary ligands, crab-like binuclear compound **2** and linear chain **45** were obtained. Although both monocarboxylates have the same monodentate coordination mode, two  $\text{NO}_2$  groups on bnb exerted steric effects to hinder the binuclear unit from the formation of 1D chains.<sup>21,46</sup> As shown in Fig. 32, when assembly of aliphatic dicarboxylates such as ox, mal, glu, and ida with  $\text{NH}_2\text{pym}$  and silver ion, compounds **40**, **85**, **107**, and **55** were isolated as 1D ladder, 2D pillared-bilayer, and 3D network with rare osb/Cmcm-C2/c topology and 1D ladder, respectively. The ox, mal, glu, and ida show  $\mu_2\text{-}\eta^1\text{:}\eta^0\text{:}\eta^1\text{:}\eta^0$ ,  $\mu_5\text{-}\eta^1\text{:}\eta^2\text{:}\eta^1\text{:}\eta^2$ ,  $\mu_2\text{-}\eta^1\text{:}\eta^0\text{:}\eta^1\text{:}\eta^0$ , and  $\mu_1\text{-}\eta^1\text{:}\eta^0\text{:}\eta^0\text{:}\eta^0$  coordination modes, respectively. The non-

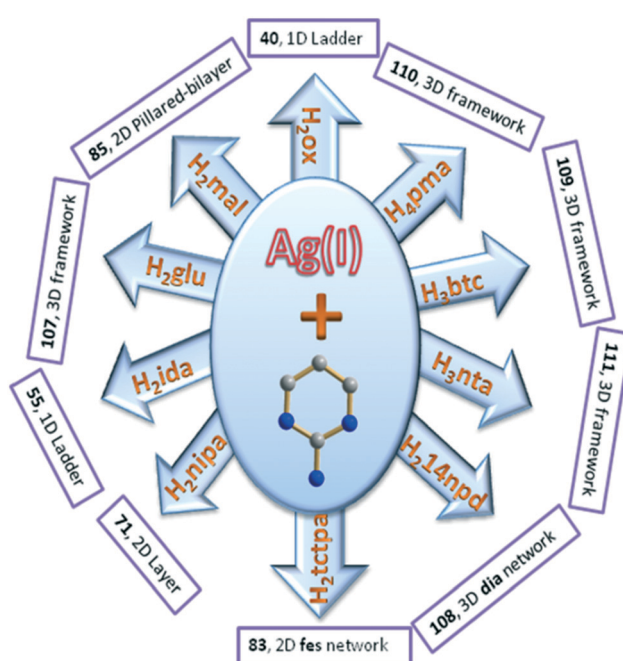


**Fig. 32** Schematic representation of polycarboxylate-controlled diverse structures with  $\text{NH}_2\text{pym}$  as main ligand.

coordinative O sites in these dicarboxylates also produce different hydrogen bonding patterns as well as other supramolecular interactions. Their conformations are also different from each other due to the free rotation of the C-C single bond. The combination of above-mentioned factors plays important roles in formation of such rich structures. When aromatic dicarboxylates such as nipa, tctpa, and 14npd are involved in assembly, compounds **71**, **83**, and **108** were isolated as 2D layered motif,<sup>54</sup> 2D fes network,<sup>57</sup> 3D dia network,<sup>43</sup> respectively. When tricarboxylate and tetracarboxylate were used, three 3D frameworks were isolated based on nta (**101**),<sup>44</sup> btc (**109**),<sup>71</sup> and pma (**110**).<sup>45</sup> In the Ag/NH<sub>2</sub>mpym/carboxylate family, totally 7 compounds are isolated depending on which carboxylates were used. In this family, aliphatic dicarboxylate (suc and glu), aromatic dicarboxylates (26npd, tpa and ipa), aliphatic tricarboxylate (nta), and aliphatic tetracarboxylate (butca) participated in construction of diverse 2D and 3D structures. The largest family of this system is Ag/NH<sub>2</sub>dmpym/carboxylates and 13 compounds are isolated based on various carboxylates. Based on above structural analysis, we found that flexible aliphatic carboxylates preferred to form low-dimensional structures, while rigid aromatic carboxylates tend to construct high-dimensional networks. With the increase in coordination groups, it also may promote the generation of 2D or 3D networks due to the increase in connectivity of the overall networks. For auxiliary carboxylates, their coordination modes, ligand conformation, number of coordination site and flexibility or rigidity influence the ligand orientation, connectivity with metal center, molecular packing and secondary interactions, which combined with aminopyrimidyl ligands synergistically dictate the final structures. That is to say, both kinds of organic ligands have to fine-tune themselves to satisfy the coordination preference of metal centers and the lower energetic arrangement in the assembly process.<sup>81</sup>

## 5. Luminescence properties of NH<sub>2</sub>pym and its derivative based coordination architectures

Coordination compounds are investigated for luminescence properties owing to (i) their higher thermal stability compared to the organic chromophores; (ii) structure diversity and modularity; (iii) the ability of tuning the emission behaviors by coordination structures; (iv) crystalline materials amenable to application development.<sup>82</sup> Various transition states have been proposed depending on structures, which include: MC (metal-centered), MLCT (metal-to-ligand charge transfer), LMCT (ligand-to-metal charge transfer), LLCT (ligand-to-ligand charge transfer), ligand-centered luminescence, and metal-to-metal charge transfer (MMCT).<sup>83</sup> In many cases, more than one transition state may be suggested.

For silver(I) coordination compounds, there is a general agreement that only weak luminescence could be observed at room temperature due to the intense spin-orbital coupling of

Ag(I),<sup>84</sup> but they are famous for the excellent emissive materials at low temperature,<sup>85</sup> with an enhanced emission intensity<sup>86</sup> and/or a shift of the emission wavelength.<sup>85</sup> Over the past decades, much evidence has accumulated to support this phenomenon that is especially pronounced for solid-state structures with argentophilic interaction. This does not mean, however, that all luminescence phenomena observed for silver compounds are necessarily due to this structural detail.<sup>87</sup> In this highlight, several examples indeed show strong emission but with argentophilic interaction at room temperature. Luminescence of Ag-aminopyrimidyl compounds normally originates from the linker rather than on the metal (LLCT), but can also involve charge transfer between linker and metal (LMCT). In them, if short Ag···Ag contacts are involved, the emission is usually found red-shifted compared to the ligands, and the phenomenon is plausibly assigned to LMCT perturbed by Ag···Ag interactions or metal-centered (MC) excited states.<sup>88</sup> Table 5 lists examples of coordination compounds selected from this highlight for which luminescence measurements have been reported. The luminescence has been observed in the solid state and at room temperature, unless noted otherwise.

Considering the luminescence of free linkers including aminopyrimidyl ligands and various carboxylates, the luminescence of carboxylates is very weak compared to that of the N-donor ligand, so the carboxylates almost have little contribution to the fluorescence emission of Ag(I)-aminopyrimidyl systems.<sup>89</sup> The N-donor ligands, such as NH<sub>2</sub>pym, NH<sub>2</sub>mpym, NH<sub>2</sub>dmpym, fapym, nfapym and ofapym, exhibit luminescence maxima of the main band located at 357 nm, 351 nm, 341 nm, 387 nm, 395 nm and 376 nm in the solid state at room temperature, respectively, which should be assigned to  $\pi^* \rightarrow \pi$  transitions. Compared to free ligand, some examples with the luminescence emission maximum did not much shift and should be assigned to LLCT. This is quite often observed for many NH<sub>2</sub>pym or its derivative based Ph<sub>3</sub>P (3, 4, 32, and 33), polycarboxylate (29, 31, 41, 46, 71, 80–85, 87, 95, and **101**) and some sulfonate (89 and 90) coordination compounds with different structures, which show ligand-centered luminescence ranging from 327 nm to 393 nm. This is commonly attributed to the  $\pi^* \rightarrow \pi$  transition and the enhanced emission intensity is generally reasoned due to increased rigidity by metal-ligand coordination. For non-mixed-ligand Ag-aminopyrimidyl compounds with small anions, almost all of them are attributed to the LLCT excitation state.

There are also some examples that their emission maximum is considerably red-shifted up to 100 nm compared to free ligands. These emission bands were often assigned to an LMCT (or MLCT) character modified by Ag···Ag interaction. The solid-state photoluminescence of **20** and **25** exhibits emission peaks at 464 and 420 nm ( $\lambda_{\text{ex}} = 330$  nm), respectively. The distinct emission behaviors of **20** and **25** should be taken into account. The emission of **25** occurs at a higher energy than that of **20** ( $\Delta_{\text{em}} = 44$  nm) which can be partially explained by existence of a shorter Ag···Ag distance (2.8852(15) Å) in **20** and hence stronger Ag···Ag interaction

**Table 5** Luminescence properties of selected compounds in this highlight

Complex	Refcode	Formula	$\lambda_{\text{ex}}/\text{nm}$	$\lambda_{\text{em}}/\text{nm}$	Assignment	Ref.
3	EXAXAD	$[\text{Ag}_2(\text{NH}_2\text{pym})_2(\text{PPh}_3)_4(\text{SO}_4)] \cdot 2\text{CH}_3\text{OH}$	440	468	LLCT	22
4	EXAXEH	$[\text{Ag}(\text{NH}_2\text{pym})_2(\text{PPh}_3)_2]\text{BF}_4$	419	448	LLCT	22
11	OJEDAJ	$[\text{Ag}_2(\text{dmoapym})_3] \cdot 2\text{CF}_3\text{SO}_3$	280	340	LLCT	26
12	OPASEE	$[\text{Ag}_2(\text{NH}_2\text{pym})_2(\text{SO}_4)(\text{dppm})_2] \cdot \text{CH}_3\text{OH}$	382	442	LLCT	27
13	POGPUTX	$[\text{Ag}_4(\text{NH}_2\text{dmpym})_6(\text{NO}_3)_4]$	280	352	LLCT	28
15	RUYKEC	$[\text{Ag}(\text{NH}_2\text{dmpym})_2(\text{ox})_{0.5}] \cdot 3\text{H}_2\text{O}$	300	396	LLCT	29
18	YOKPUK	$[\text{Ag}_2(\text{NH}_2\text{dmpym})_2] \cdot 2\text{ClO}_4$	280	345	LLCT	32
20	IZECUM	$[\text{Ag}_4(\text{NHpym})_2(\text{dppm})_2] \cdot 2\text{ClO}_4 \cdot 2\text{DMF}$	330	464	LMCT mixed with argentophilic interaction	34
21	KEXFUP	$[\text{Ag}_2(\text{dpyapym}-2)_2] \cdot 2\text{NO}_3$	367	468	LLCT	35
25	UYURAI	$[\text{Ag}_6(\text{NHdmpym})_2(\text{dppm})_4] \cdot 4\text{ClO}_4$	330	420	LMCT mixed with argentophilic interaction	34
26	GEZVOY	$[\text{Ag}(\text{nfapym})\text{ClO}_4]_n$	300	461	LLCT	40
27	GEZVUE	$[\text{Ag}(\text{nfapym})\text{CF}_3\text{SO}_3 \cdot \text{EtOH}]_n$	300	418	LLCT	40
28	GEZWAL	$[\text{Ag}(\text{nfapym})\text{CF}_3\text{CO}_2]_n$	300	445	LLCT	40
29	GEZVEO	$[\text{Ag}(\text{nfapym})\text{NO}_3]_n$	300	445	LLCT	40
30	GEZWUF	$[\text{Ag}(\text{ofapym})\text{CF}_3\text{SO}_3 \cdot \text{EtOH}]_n$	300	376, 520	LLCT and/or LMCT	40
31	EPICEM	$[\text{Ag}_2(\text{NH}_2\text{dmpym})_4(\text{mal}) \cdot \text{H}_2\text{O}]_n$	320	353	LLCT	41
32	EXAWOQ	$[\text{Ag}_4(\text{NO}_3)_4(\text{PPh}_3)_4(\text{NH}_2\text{pym})_2]_n$	442	471	LLCT	22
33	EXAWUW	$[\text{Ag}_4(\text{Ac})_4(\text{PPh}_3)_4(\text{NH}_2\text{pym})_2]_n$	440	468	LLCT	22
39	KEXFID	$[\text{Ag}_2(\text{dpyapym}-1)_2]_n \cdot 2n\text{NO}_3$	367	468	LLCT	35
41	ILAFOR	$[\text{Ag}_2(\text{NH}_2\text{dmpym})_3(\text{Hnta})]_n$	300	358	LLCT	44
42	KEXFEZ	$[\text{Ag}(\text{dpyapym}-2)]_n \cdot n\text{CF}_3\text{SO}_3$	358	467	LLCT	35
43	KEXFOJ	$[\text{Ag}_2(\text{dpyapym}-2)(\text{SCN})_2]_n \cdot n\text{H}_2\text{O}$	358	485	LLCT	35
44	LURCUX	$[\text{Ag}_4(\text{NH}_2\text{dmpym})_4(\text{pma}) \cdot (\text{H}_2\text{O})_2]_n \cdot 6n\text{H}_2\text{O}$	310	450	LMCT mixed with MC (d-s/d-p)	45
46	MUTJER	$[\text{Ag}_4(\text{NH}_2\text{dmpym})_6(\text{butca}) \cdot 2\text{H}_2\text{O}]_n$	330	360	LLCT	47
49	OJECUC	$[\text{Ag}_2(\text{NH}_2\text{mompym})_2(\text{CF}_3\text{SO}_3)_2]_n$	280	346	LLCT	26
50	OJEDEN	$[\text{Ag}(\text{dmoapym})(\text{CF}_3\text{CO}_2)]_n$	280	336	LLCT	26
51	POGQAE	$[\text{Ag}(\text{NH}_2\text{pym})(\text{NO}_3)]_n$	280	360	LLCT	28
52	POGQEI	$[\text{Ag}(\text{NH}_2\text{mompym})(\text{NO}_3)]_n$	280	338	LLCT	28
53	POGQIM	$[\text{Ag}(\text{dmoapym})(\text{NO}_3)]_n$	280	336	LLCT	28
59	UNEKAA	$[\text{Ag}(\text{fapym})(\text{CO}_2\text{CF}_3)]_n$	354	390, 502	N/A	50
60	UNEKEE	$[\text{Ag}(\text{fapym})(\text{SO}_3\text{CF}_3) \cdot \text{EtOH}]_n$	355	377 481	N/A	50
61	UNEKII	$[\text{Ag}(\text{fapym})(\text{SO}_3\text{CF}_3) \cdot \text{PrOH}]_n$	N/A	375	N/A	50
67	WUXJEF	$[\text{Ag}(\text{NH}_2\text{mpym})_2(26\text{npd})_{0.5} \cdot \text{H}_2\text{O}]_n$	330	423	LMCT	51
69	YOKPIY	$[\text{Ag}_4(\text{NH}_2\text{dmpym})_4(\text{CF}_3\text{CO}_2)_4]_n$	280	350	LLCT	32
70	YOKPOE	$[\text{Ag}(\text{NH}_2\text{dmpym})(\text{CF}_3\text{SO}_3)(\text{H}_2\text{O})]_n$	280	354	LLCT	32
71	GUPXEV	$[\text{Ag}_2(\text{NH}_2\text{pym})_1 \cdot 5(\text{nipa}) \cdot \text{H}_2\text{O}]_n$	330	400	LLCT	54
72	YOKQEV	$[\text{Ag}(\text{dmoapym})(\text{ClO}_4)]_n$	280	334	LLCT	32
73	HOGCEM	$[\text{Ag}_3(\text{dmoapym})_3(\text{NO}_3)_3]_n$	280	336	LLCT	28
75	YOKQAR	$[\text{Ag}(\text{NH}_2\text{mompym})(\text{ClO}_4)]_n$	280	342	LLCT	32
76	GEZWQZ	$[\text{Ag}(\text{ofapym})\text{ClO}_4]_n$	300	378, 515	LLCT and/or LMCT	40
77	GEZXAM	$[\text{Ag}(\text{ofapym})\text{CF}_3\text{CO}_2]_n$	300	393, 469	LLCT	40
78	GEZWIT	$[\text{Ag}(\text{ofapym})\text{NO}_3]_n$	300	383, 510	LLCT and/or LMCT	40
79	GEZVIS	$[\text{Ag}(\text{nfapym})\text{NO}_3]_n$	300	560	LMCT	40
80	GUPXIZ	$[\text{Ag}_2(\text{NH}_2\text{dmpym})_2(\text{nipa})]_n$	330	432	LLCT	54
81	FIJXON	$[\text{Ag}_2(\text{NH}_2\text{dmpym})_2(26\text{npd})]_n$	330	418	LLCT	55
83	BANMEK	$[\text{Ag}_4(\text{NH}_2\text{pym})_4(\text{tcpa})_2]_n$	330	463	LLCT	57
84	BANMIO	$[\text{Ag}_2(\text{NH}_2\text{dmpym})(\text{tcpa})]_n$	330	471	LLCT	57
85	EPICAI	$[\text{Ag}_3(\text{NH}_2\text{pym})_3(\text{mal})\text{NO}_3]_n$	320	367	LLCT	41
86	ILAFL	$[(\text{NH}_4)\text{Ag}_2(\text{NH}_2\text{mpym})(\text{nta}) \cdot 3\text{H}_2\text{O}]_n$	300	470	LMCT mixed with MC (d-s/d-p)	44
87	LALDIN	$[\text{Ag}_2(\text{NH}_2\text{dmpym})_2(\text{suc}) \cdot \text{H}_2\text{O}]_n$	320	369	LLCT	58
88	MUTJAN	$\{[\text{Ag}_4(\text{NH}_2\text{mpym})_2(\text{butca})(\text{H}_2\text{O})_4] \cdot 2\text{H}_2\text{O}\}_n$	330	487	LMCT mixed with MC (d-s/d-p)	47
89	OKOVOA	$[\text{Ag}(\text{NH}_2\text{pym})(\text{nds})_{0.5}]_n$	330	374	LLCT	59
90	OKOVUG	$[\text{Ag}(\text{NH}_2\text{dmpym})(\text{nds})_{0.5}]_n$	330	356	LLCT	59
91	OPANEZ	$[\text{Ag}(\text{NH}_2\text{dmpym})(\text{tpa})_{1/2}]_n$	300	483	Mixed LLCT and/or LMCT	60
92	RUYJIF	$[\text{Ag}(\text{NH}_2\text{mpym})(\text{suc})_{0.5} \cdot 0.5\text{H}_2\text{O}]_n$	300	513	LMCT mixed with MC (d-s/d-p)	29
93	RUYJOL	$[\text{Ag}_2(\text{NH}_2\text{mpym})_2(\text{glu})_3 \cdot 1.5\text{H}_2\text{O}]_n$	300	518	LMCT mixed with MC (d-s/d-p)	29
94	RUYKAY	$[\text{Ag}_2(\text{NH}_2\text{mpym})_2(\text{tpa})(\text{H}_2\text{O})]_n$	300	533	LMCT mixed with MC (d-s/d-p)	29
95	RUYKIG	$[\text{Ag}(\text{NH}_2\text{dmpym})(\text{bbdc})_{0.5} \cdot 0.5\text{H}_2\text{O}]_n$	300	393	LLCT	29
101	ILAFEH	$[\text{Ag}_{1.5}(\text{NH}_2\text{pym})(\text{nta})_{0.5}]_n$	300	376	LLCT	44
102	LALDOT	$[\text{Ag}_2(\text{NH}_2\text{dmpym})_2(\text{ipa}) \cdot 2\text{H}_2\text{O}]_n$	380	467	LMCT mixed with MC (d-s/d-p)	58
103	RUYJUR	$[\text{Ag}_2(\text{NH}_2\text{mpym})_2(\text{ipa}) \cdot 2\text{H}_2\text{O}]_n$	300	515	LMCT mixed with MC (d-s/d-p)	29
106	OPANAV	$[\text{Ag}(\text{NH}_2\text{dmpym})(\text{btc})_{1/3}]_n$	300	453	Mixed LLCT and/or LMCT	60
109	GUKQIN	$[\text{Ag}_3(\text{NH}_2\text{pym})_2(\text{btc})]_n$	383	464	LMCT mixed with MC (d-s/d-p)	71
110	LURCOR	$[\text{Ag}_4(\text{NH}_2\text{pym})_2(\text{pma}) \cdot (\text{H}_2\text{O})_2]_n$	320	505	LMCT mixed with MC (d-s/d-p)	45

which has important influence on the photoluminescence properties of this kind of complexes. The emitting transition states of **20** and **25** could be tentatively assigned to the ligand-to-metal charge transfer (LMCT) transition which also is probably mixed with a metal-centered transition state modified by Ag $\cdots$ Ag interaction (Fig. 33).

The emission above *ca.* 500 nm is often attributed to charge transfer phenomena, LMCT (or MLCT) modified by MC (d-s/d-p) states incorporating Ag $\cdots$ Ag interactions. For mixed-ligand coordination compound **92–94** and **103**, low-energy emissions were observed. Intense emissions are observed at 513 nm for **92**, 518 nm for **93**, 533 nm for **94**, and 515 nm for **103**, respectively under the excitation of 300 nm. Compared to the emission of the corresponding N-donor ligands, the emission bands of **92–94** and **103** are red-shifted by more than 150 nm, which should be assigned to ligand-to-metal charge transfer (LMCT), mixed with metal-centered (d-s/d-p) transitions (Fig. 34).

Thermochromic luminescence<sup>90</sup> was also firstly observed in **109**, which emits blue luminescence with a maximum at 464 nm upon excitation at 383 nm at room temperature. Interestingly, when cooling to cryogenic temperature of 77 K, the bathochromic emission of **109** occurred at 488 nm (Fig. 35). The presence of the red shift ( $\Delta = 24$  nm) in the solid-state emission maximum of **109** upon cooling is consistent with what has been observed in other luminescent poly-nuclear silver compounds with Ag $\cdots$ Ag interactions.<sup>91</sup> In **109**, abundant Ag $\cdots$ Ag contacts including strong ( $d_{\text{Ag}\cdots\text{Ag}}$  equal to or shorter than 2.89 Å) and weak ( $d_{\text{Ag}\cdots\text{Ag}}$  longer than 2.89 Å but still shorter than 3.44 Å) interactions that fall in the range of 2.786(2)–3.253(3) Å are observed and the thermal compression of Ag $\cdots$ Ag distance may occur when cooling, which is responsible for the red-shift of LMCT transition, suggesting that cluster-centered emission was populated at lower temperature. Thus, the observed luminescence of **109** should be related to the existence of the argentophilicity-supported silver chains and assigned to ligand-to-metal charge transfer (LMCT) and excited state of pure d-s origin modified by Ag $\cdots$ Ag interaction.

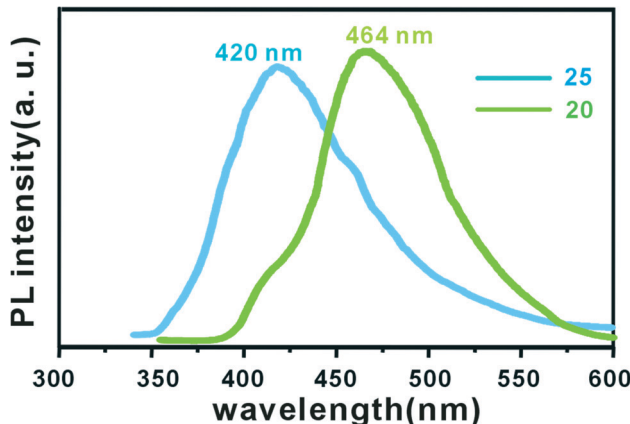


Fig. 33 Luminescence spectra of **20** and **25** under the excitation of 330 nm at room temperature.

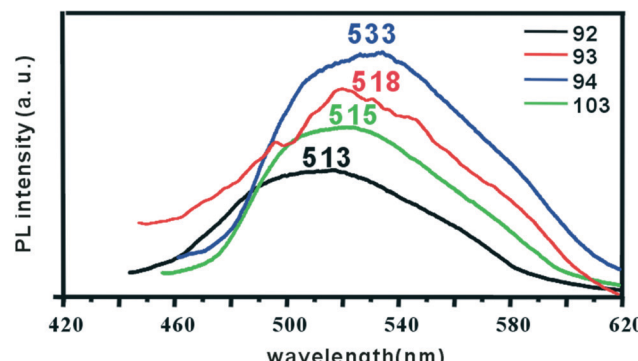


Fig. 34 Luminescence spectra of **92–94** and **103** under the excitation of 300 nm at room temperature.

## 6. Conclusions

The purpose of this highlight is to illustrate the current advances of Ag(i)-aminopyrimidyl coordination compounds in fields of coordination chemistry and crystal engineering. To date, it has been witnessed the important advances in structural diversity of Ag(i) aminopyrimidyl coordination compounds. Thus, the overall structure summary and a better understanding of various factors such as anion, solvent, substituents and so on in influencing their assembly will be of great importance. Totally 110 X-ray-structure-characterized Ag(i)-aminopyrimidyl coordination compounds were outlined and the influence factors that dictate their formation were discussed in detail. These factors generally contributed largely to their crystal growth, structural assemblies, dynamic transformations, and luminescent properties in a complicated but highly effective manner. Nevertheless, the detailed assembly mechanism influenced by so many factors is still hard to specify and most statements about these are usually based on compared experiments. So, it is expected to obtain more and more experimental facts in this issue in order to further understand the assembly as well as the structure-

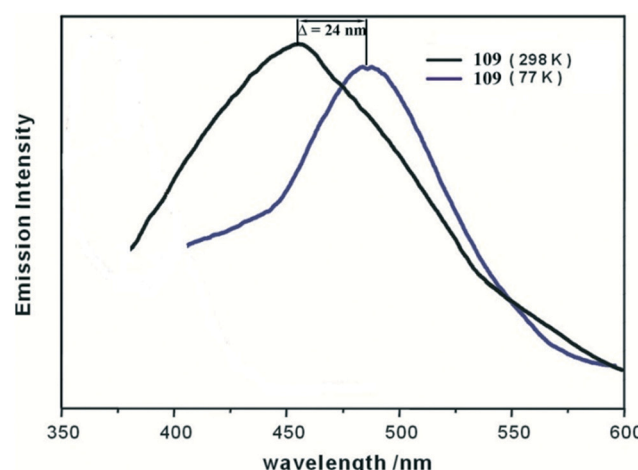


Fig. 35 Luminescence spectra of **109** under the excitation of 383 nm at room temperature and 77 K.

property associations. Current preliminary but indispensable progress based on these compounds should also provide precious experiences to promote this subfield to go ahead. We will be going to devote time to this field including the collection of more related data and the development of a new theory even beyond simple host-guest interaction and classic coordination chemistry.

## Acknowledgements

This work was supported by the NSFC (grant no. 21201110) and the Research Award Fund for Outstanding Middle-aged and Young Scientist of Shandong Province (BS2013CL010). X. P.W. thanks the Youth Award of Shandong Province (grant no. 2007BS03033) for financial assistance. T.P.H. thanks the International Science & Technology Cooperation Program of China (no. 2011DFA51980) for financial assistance.

## References

- (a) Y. Cui, Y. Yue, G. Qian and B. Chen, *Chem. Rev.*, 2011, **112**, 1126; (b) L. E. Kreno, K. Leong, O. K. Farha, M. Allendorf, R. P. Van Duyne and J. T. Hupp, *Chem. Rev.*, 2011, **112**, 1105; (c) J.-R. Li, J. Sculley and H.-C. Zhou, *Chem. Rev.*, 2011, **112**, 869; (d) M. P. Suh, H. J. Park, T. K. Prasad and D.-W. Lim, *Chem. Rev.*, 2011, **112**, 782; (e) J.-P. Zhang, Y.-B. Zhang, J.-B. Lin and X.-M. Chen, *Chem. Rev.*, 2011, **112**, 1001; (f) M. J. Zaworotko, *Chem. Soc. Rev.*, 1994, **23**, 283; (g) A. Dhakshinamoorthy and H. Garcia, *Chem. Soc. Rev.*, 2014, **43**, 5750; (h) Y. He, B. Li, M. O'Keeffe and B. Chen, *Chem. Soc. Rev.*, 2014, **43**, 5618; (i) P. Ramaswamy, N. E. Wong and G. K. H. Shimizu, *Chem. Soc. Rev.*, 2014, **43**, 5913; (j) A. Schneemann, V. Bon, I. Schwedler, I. Senkovska, S. Kaskel and R. A. Fischer, *Chem. Soc. Rev.*, 2014, **43**, 6062; (k) V. Stavila, A. A. Talin and M. D. Allendorf, *Chem. Soc. Rev.*, 2014, **43**, 5994; (l) Z. M. Zhang, Y. G. Li, S. Yao, E. B. Wang, Y. H. Wang and R. Clerac, *Angew. Chem., Int. Ed.*, 2009, **48**, 1581; (m) Z. M. Zhang, S. Yao, Y. G. Li, H. H. Wu, Y. H. Wang, M. Rouzieres, R. Clerac, Z. M. Su and E. B. Wang, *Chem. Commun.*, 2013, **49**, 2515; (n) F. J. Ma, S. X. Liu, C. Y. Sun, D. D. Liang, G. J. Ren, F. Wei, Y. G. Chen and Z. M. Su, *J. Am. Chem. Soc.*, 2011, **133**, 4178; (o) W. L Leong and J. J. Vittal, *Chem. Rev.*, 2011, **111**, 688; (p) M. Kurmoo, *Chem. Soc. Rev.*, 2009, **38**, 1353.
- (a) R.-Q. Zou, R.-Q. Zhong, M. Du, T. Kiyobayashi and Q. Xu, *Chem. Commun.*, 2007, 2467; (b) Z. Yin, Q.-X. Wang and M.-H. Zeng, *J. Am. Chem. Soc.*, 2012, **134**, 4857; (c) M.-H. Zeng, Q.-X. Wang, Y.-X. Tan, S. Hu, H.-X. Zhao, L.-S. Long and M. Kurmoo, *J. Am. Chem. Soc.*, 2010, **132**, 2561; (d) S. M. Neville, G. J. Halder, K. W. Chapman, M. B. Duriska, P. D. Southon, J. D. Cashion, J. F. Letard, B. Moubaraki, K. S. Murray and C. J. Kepert, *J. Am. Chem. Soc.*, 2008, **130**, 2869; (e) H. Wu, J. Yang, Z.-M. Su, S. R. Batten and J.-F. Ma, *J. Am. Chem. Soc.*, 2011, **133**, 11406; (f) K. V. Domasevitch, I. Boldog, E. B. Rusanov, A. N. Chernega and J. Sieler, *Angew. Chem., Int. Ed.*, 2001, **40**, 3435; (g) Y. Takashima, V. M. Martinez, S. Furukawa, M. Kondo, S. Shimomura, H. Uehara, M. Nakahama, K. Sugimoto and S. Kitagawa, *Nat. Commun.*, 2011, **2**, 168.
- (a) D. Zhao, D. J. Timmons, D. Yuan and H.-C. Zhou, *Acc. Chem. Res.*, 2011, **44**, 123; (b) T. T. Luo, H. C. Wu, Y. C. Jao, S. M. Huang, T. W. Tseng, Y. S. Wen, G. H. Lee, S. M. Peng and K. L. Lu, *Angew. Chem., Int. Ed.*, 2009, **48**, 9461; (c) X. Zhao, F. Liu, L. Zhang, D. Sun, R. Wang, Z. Ju, D. Yuan and D. Sun, *Chem. – Eur. J.*, 2014, **20**, 649; (d) J. Sun, D. Sun, S. Yuan, D. X. Tian, L. L. Zhang, X. P. Wang and D. F. Sun, *Chem. – Eur. J.*, 2012, **18**, 16525; (e) X. Bao, H. J. Shepherd, L. Salmon, G. Molnar, M. L. Tong and A. Bousseksou, *Angew. Chem., Int. Ed.*, 2013, **52**, 1198; (f) Y. B. Zhang, H. L. Zhou, R. B. Lin, C. Zhang, J. B. Lin, J. P. Zhang and X. M. Chen, *Nat. Commun.*, 2012, **3**, 642.
- (a) W. E. Hunt, C. H. Schwalbe, K. Bird and P. D. Mallinson, *Biochem. J.*, 1980, **187**, 533; (b) B. R. Baker and D. V. Santi, *J. Pharm. Sci.*, 1965, **54**, 1252.
- Y. H. Wang, K. L. Chu, H. C. Chen, C. W. Yeh, Z. K. Chan, M. C. Suen, J. D. Chen and J. C. Wang, *CrystEngComm*, 2006, **8**, 84.
- D. Sun, G.-G. Luo, R.-B. Huang, N. Zhang and L.-S. Zheng, *Acta Crystallogr., Sect. C: Cryst. Struct. Commun.*, 2009, **65**, m305.
- C. Y. Lin, Z. K. Chan, C. W. Yeh, C. J. Wu, J. D. Chen and J. C. Wang, *CrystEngComm*, 2006, **8**, 841.
- M. C. Etter and D. A. Adsmond, *J. Chem. Soc., Chem. Commun.*, 1990, 589.
- M. S. Driver and J. F. Hartwig, *J. Am. Chem. Soc.*, 1996, **118**, 4206.
- K. Kobayashi, T. Shirasaka, K. Yamaguchi, S. Sakamoto, E. Horn and N. Furukawa, *Chem. Commun.*, 2000, 41.
- R. Weiss and H. Venner, *Hoppe-Seyler's Z. Physiol. Chem.*, 1969, **350**, 396.
- A. N. Khlobystov, A. J. Blake, N. R. Champness, D. A. Lemenovskii, A. G. Majouga, N. V. Zyk and M. Schröder, *Coord. Chem. Rev.*, 2001, **222**, 155.
- (a) F. H. Allen, *Acta Crystallogr., Sect. B: Struct. Sci.*, 2002, **58**, 380; (b) Cambridge Structure Database search, CSD Version 5.35 (November 2013) with 3 updates (Nov 2013, Feb 2014 and May 2014).
- G. Smith, B. A. Cloutt, D. E. Lynch, K. A. Byriel and C. H. L. Kennard, *Inorg. Chem.*, 1998, **37**, 3236.
- K. Brandenburg, 2008, DIAMOND. Version 3.1f. Crystal Impact GbR, Bonn, Germany.
- K. M. Fromm, J. L. Sague and A. Y. Robin, *Inorg. Chim. Acta*, 2013, **403**, 2.
- (a) A. Y. Robin and K. M. Fromm, *Coord. Chem. Rev.*, 2006, **250**, 2127; (b) Z. Yan, J. Y. Li, T. Liu, Z. P. Ni, Y. C. Chen, F. S. Guo and M. L. Tong, *Inorg. Chem.*, 2014, **53**, 8129; (c) R. Banerjee, A. Phan, B. Wang, C. Knobler, H. Furukawa, M. O'Keeffe and O. M. Yaghi, *Science*, 2008, **319**, 939; (d) X. M. Chen and M. L. Tong, *Acc. Chem. Res.*, 2007, **40**, 162; (e) J. Li, Y. Guo, H. R. Fu, J. Zhang, R. B. Huang, L. S. Zheng and J. Tao, *Chem. Commun.*, 2014, **50**, 9161; (f) S. Cundy and P. A. Cox, *Chem. Rev.*, 2003, **103**, 663;

- (g) X. Wang and Y. D. Li, *J. Am. Chem. Soc.*, 2002, **124**, 2880; (h) B. Zheng, H. Dong, J. F. Bai, Y. Z. Li, S. H. Li and M. Scheer, *J. Am. Chem. Soc.*, 2008, **130**, 7778; (i) B. Xu, X. Lin, Z. Z. He, Z. J. Lin and R. Cao, *Chem. Commun.*, 2011, **47**, 3766; (j) J.-P. Zhao, Q. Yang, Z.-Y. Liu, R. Zhao, B.-W. Hu, M. Du, Z. Chang and X.-H. Bu, *Chem. Commun.*, 2012, **48**, 6568; (k) J. Yu, Y. Cui, C. Wu, Y. Yang, Z. Wang, M. O'Keeffe, B. Chen and G. Qian, *Angew. Chem., Int. Ed.*, 2012, **51**, 10542; (l) T. Han, W. Shi, Z. Niu, B. Na and P. Cheng, *Chem. - Eur. J.*, 2013, **19**, 994.
- 18 (a) S.-L. Zheng, A. Volkov, C. L. Nygren and P. Coppens, *Chem. - Eur. J.*, 2007, **13**, 8583; (b) G. Smith, A. N. Reddy, K. A. Byriel and C. H. L. Kennard, *J. Chem. Soc., Dalton Trans.*, 1995, 3565; (c) P. Nockemann and G. Meyer, *Z. Anorg. Allg. Chem.*, 2002, **628**, 1636; (d) P. Woidy and F. Kraus, *Z. Anorg. Allg. Chem.*, 2013, **639**, 2643; (e) D. Sun, F. J. Liu, R. B. Huang and L. S. Zheng, *CrystEngComm*, 2013, **15**, 1185.
- 19 D. Sun, G.-G. Luo, N. Zhang, Z.-H. Wei, C.-F. Yang, R.-B. Huang and L.-S. Zheng, *Chem. Lett.*, 2010, **39**, 190.
- 20 H. Yang, *Acta Crystallogr., Sect. E: Struct. Rep. Online*, 2009, **65**, m1177.
- 21 Y.-G. Li, Q.-B. Jiang, K. Cheng, H. Yan and H.-L. Zhu, *Z. Anorg. Allg. Chem.*, 2009, **635**, 2572.
- 22 L.-N. Cui, K.-Y. Hu, Q.-H. Jin, Z.-F. Li, J.-Q. Wu and C.-L. Zhang, *Polyhedron*, 2011, **30**, 2253.
- 23 C.-J. Wu, C.-Y. Lin, P.-C. Cheng, C.-W. Yeh, J.-D. Chen and J.-C. Wang, *Polyhedron*, 2011, **30**, 2260.
- 24 I. Stoll, R. Brodbeck, B. Neumann, H.-G. Stammler and J. Mattay, *CrystEngComm*, 2009, **11**, 306.
- 25 H.-L. Yang, S. Yang, X.-Y. Qiu, S.-C. Shao, J.-L. Ma, L. Sun and H.-L. Zhu, *Z. Kristallogr. - New Cryst. Struct.*, 2004, **219**, 157.
- 26 G.-G. Luo, D. Sun, N. Zhang, R.-B. Huang and L.-S. Zheng, *J. Mol. Struct.*, 2009, **938**, 65.
- 27 Q.-H. Jin, L.-L. Song, K.-Y. Hu, L.-L. Zhou, Y.-Y. Zhang and R. Wang, *Inorg. Chem. Commun.*, 2010, **13**, 62.
- 28 G.-G. Luo, R.-B. Huang, N. Zhang, L.-R. Lin and L.-S. Zheng, *Polyhedron*, 2008, **27**, 3231.
- 29 D. Sun, N. Zhang, R.-B. Huang and L.-S. Zheng, *Cryst. Growth Des.*, 2010, **10**, 3699.
- 30 H.-L. Zhu, S. Yang, J.-L. Ma, X.-Y. Qiu, L. Sun and S.-C. Shao, *Acta Crystallogr., Sect. E: Struct. Rep. Online*, 2003, **59**, m1046.
- 31 D. Sun, H.-J. Hao, F.-J. Liu, H.-F. Su, R.-B. Huang and L.-S. Zheng, *CrystEngComm*, 2012, **14**, 480.
- 32 G.-G. Luo, R.-B. Huang, J.-H. Chen, L.-R. Lin and L.-S. Zheng, *Polyhedron*, 2008, **27**, 2791.
- 33 H. Yang, *Acta Crystallogr., Sect. E: Struct. Rep. Online*, 2009, **65**, m1176.
- 34 D. Sun, N. Zhang, R.-B. Huang and L.-S. Zheng, *Inorg. Chem. Commun.*, 2011, **14**, 1039.
- 35 Y.-N. Chi, K.-L. Huang, F.-Y. Cui, Y.-Q. Xu and C.-W. Hu, *Inorg. Chem.*, 2006, **45**, 10605.
- 36 D. Sun, G.-G. Luo, N. Zhang, R.-B. Huang and L.-S. Zheng, *Chem. Commun.*, 2011, **47**, 1461.
- 37 R. Stewart and M. G. Harris, *J. Org. Chem.*, 1978, **43**, 3123.
- 38 F. L. Liu, Z. H. Xu, X. Y. Zhang, X. P. Wang and D. Sun, *Chem. - Asian J.*, 2014, **9**, 452.
- 39 A. G. Young and L. R. Hanton, *Coord. Chem. Rev.*, 2008, **252**, 1346.
- 40 J. Eberhard, I. Stoll, R. Brockhinke, B. Neumann, H.-G. Stammler, A. Riefer, E. Rauls, W. G. Schmidt and J. Mattay, *CrystEngComm*, 2013, **15**, 4225.
- 41 D. Sun, N. Zhang, Q.-J. Xu, G.-G. Luo, R.-B. Huang and L.-S. Zheng, *J. Mol. Struct.*, 2010, **970**, 134.
- 42 L. Chen and M. Hong, *Design and Construction of Coordination Polymers*, 2009, J.Wiley & Sons, Hoboken USA.
- 43 D. Sun, G.-G. Luo, N. Zhang, J.-H. Chen, R.-B. Huang, L.-R. Lin and L.-S. Zheng, *Polyhedron*, 2009, **28**, 2983.
- 44 D. Sun, N. Zhang, Q.-J. Xu, Z.-H. Wei, R.-B. Huang and L.-S. Zheng, *Inorg. Chim. Acta*, 2011, **368**, 67.
- 45 D. Sun, N. Zhang, G.-G. Luo, Q.-J. Xu, R.-B. Huang and L.-S. Zheng, *Polyhedron*, 2010, **29**, 1842.
- 46 Z.-L. You and H.-L. Zhu, *Acta Crystallogr., Sect. C: Cryst. Struct. Commun.*, 2004, **60**, m623.
- 47 D. Sun, N. Zhang, Q.-J. Xu, R.-B. Huang and L.-S. Zheng, *J. Mol. Struct.*, 2010, **975**, 17.
- 48 A. W. Xu, C. Y. Su, Z. F. Zhang, Y. P. Cai and C. L. Chen, *New J. Chem.*, 2001, **25**, 479.
- 49 Q.-H. Jin, X.-L. Xin, X.-Y. Ci and K.-B. Yu, *Acta Crystallogr., Sect. C: Cryst. Struct. Commun.*, 2002, **58**, m174.
- 50 I. Stoll, R. Brockhinke, A. Brockhinke, M. Bottcher, T. Koop, H. G. Stammler, B. Neumann, A. Niemeyer, A. Hutten and J. Mattay, *Chem. Mater.*, 2010, **22**, 4749.
- 51 D. Sun, N. Zhang, Q.-J. Xu, R.-B. Huang and L.-S. Zheng, *J. Organomet. Chem.*, 2010, **695**, 1598.
- 52 Q.-H. Jin, H.-G. Zheng, X.-L. Xin, X.-Y. Ci and K.-B. Yu, *Z. Kristallogr. - New Cryst. Struct.*, 2002, **217**, 341.
- 53 (a) A. Erxleben, *Inorg. Chem.*, 2001, **40**, 2928; (b) Z. Shi, S. H. Feng, S. Gao, L. R. Zhang, G. Y. Yang and J. Hua, *Angew. Chem., Int. Ed.*, 2000, **39**, 2325; (c) M. J. Hannon, C. L. Painting and N. W. Alcock, *Chem. Commun.*, 1999, 2023; (d) G. Baum, E. C. Constable, D. Fenske, C. E. Housecroft and T. Kulke, *Chem. - Eur. J.*, 1995, **5**, 1862; (e) G. Struckmeier, U. Therwalt and J. H. Fuhrhop, *J. Am. Chem. Soc.*, 1976, **98**, 278; (f) K. T. Potts, M. Keshavarz-K, F. S. Tham, K. A. Gheysen Raiford, C. Arana and H. D. Abruna, *Inorg. Chem.*, 1993, **32**, 5477.
- 54 D. Sun, G.-G. Luo, N. Zhang, Z.-H. Wei, C.-F. Yang, Q.-J. Xu, R.-B. Huang and L.-S. Zheng, *J. Mol. Struct.*, 2010, **967**, 147.
- 55 D. Sun, S. Yuan, S. S. Liu, Y. Q. Zhao, L. L. Han and X. P. Wang, *Z. Naturforsch., B: J. Chem. Sci.*, 2013, **68**, 357.
- 56 G. G. Luo, D. Sun, N. Zhang, R. B. Huang and L. S. Zheng, *Acta Crystallogr., Sect. C: Cryst. Struct. Commun.*, 2009, **65**, M377.
- 57 D. Sun, R. B. Huang and L. S. Zheng, *Z. Naturforsch., B: J. Chem. Sci.*, 2011, **66**, 1035.
- 58 D. Sun, Q.-J. Xu, C.-Y. Ma, N. Zhang, R.-B. Huang and L.-S. Zheng, *CrystEngComm*, 2010, **12**, 4161.
- 59 D. Sun, N. Zhang, Z.-H. Wei, C.-F. Yang, R.-B. Huang and L.-S. Zheng, *J. Mol. Struct.*, 2010, **981**, 80.
- 60 G.-G. Luo, D. Sun, N. Zhang, Q.-J. Xu, L.-R. Lin, R.-B. Huang and L.-S. Zheng, *Inorg. Chem. Commun.*, 2010, **13**, 10.

- 61 J. Wang, J.-G. Wang, X.-H. Li and H.-P. Xiao, *Transition Met. Chem.*, 2013, **38**, 765.
- 62 C. Janiak, *J. Chem. Soc., Dalton Trans.*, 2000, 3885.
- 63 (a) P. Pyykko, *Chem. Rev.*, 1997, **97**, 597; (b) C.-M. Che, M.-C. Tse, M. C. W. Chan, K.-K. Cheung, D. L. Phillips and K.-H. Leung, *J. Am. Chem. Soc.*, 2000, **122**, 2464; (c) Y. B. Dong, J. Y. Cheng, R. Q. Huang, M. D. Smith and H. C. zur Loya, *Inorg. Chem.*, 2003, **42**, 5699; (d) J. P. Lang, S. J. Ji, Q. F. Xu, Q. Shen and K. Tatsumi, *Coord. Chem. Rev.*, 2003, **241**, 47; (e) H. L. Cui, S. Z. Zhan, M. A. Li, S. W. Ng and D. Li, *Dalton Trans.*, 2011, **40**, 6490; (f) X. F. Kuang, X. Y. Wu, R. M. Yu, J. P. Donahue, J. S. Huang and C. Z. Lu, *Nat. Chem.*, 2010, **2**, 461; (g) F. F. Li, J. F. Ma, S. Y. Song, J. Yang, H. Q. Jia and N. H. Hu, *Cryst. Growth Des.*, 2006, **6**, 209.
- 64 A. Addison, T. N. Rao, J. Reedijk, J. van Rijn and G. C. Verschoor, *J. Chem. Soc., Dalton Trans.*, 1984, 1349.
- 65 L. Yang, D. R. Powell and R. P. Houser, *Dalton Trans.*, 2007, 955.
- 66 D. Cremer and J. A. Pople, *J. Am. Chem. Soc.*, 1975, **97**, 1354.
- 67 J. Bernstein, R. E. Davis, L. Shimon and N. L. Chang, *Angew. Chem., Int. Ed. Engl.*, 1995, **35**, 1555.
- 68 (a) V. A. Blatov, M. O'Keeffe and D. M. Proserpio, *CrystEngComm*, 2010, **12**, 44; (b) I. A. Baburin, V. A. Blatov, L. Carlucci, G. Cianib and D. M. Proserpio, *CrystEngComm*, 2008, **10**, 1822; (c) I. A. Baburin, V. A. Blatov, L. Carlucci, G. Cianib and D. M. Proserpio, *Cryst. Growth Des.*, 2008, **8**, 519.
- 69 (a) K. A. Hirsch, S. R. Wilson and J. S. Moore, *Inorg. Chem.*, 1997, **36**, 2960; (b) S. R. Batten, B. F. Hoskins and R. Robson, *Chem. – Eur. J.*, 2000, **6**, 156.
- 70 (a) P. Jensen, D. J. Price, S. R. Batten, B. Moubaraki and K. S. Murray, *Chem. – Eur. J.*, 2000, **6**, 3186; (b) D. L. Long, R. J. Hill, A. J. Blake, N. R. Champness, P. Hubberstey, C. Wilson and M. Schroder, *Chem. – Eur. J.*, 2005, **11**, 1384; (c) L. Carlucci, G. Ciani and D. M. Proserpio, *Coord. Chem. Rev.*, 2003, **246**, 247; (d) R. L. LaDuca, *Coord. Chem. Rev.*, 2009, **293**, 1759; (e) M. Bi, G. Li, Y. Zou, Z. Shi and S. Feng, *Inorg. Chem.*, 2007, **46**, 604.
- 71 G.-G. Luo, D. Sun, Q.-J. Xu, N. Zhang, R.-B. Huang, L. Lin and L.-S. Zheng, *Inorg. Chem. Commun.*, 2009, **12**, 436.
- 72 R. G. Pearson, *J. Am. Chem. Soc.*, 1963, **85**, 3533.
- 73 V. A. Blatov, A. P. Shevchenko and D. M. Proserpio, *Cryst. Growth Des.*, 2014, **14**, 3576; <http://topospro.com>.
- 74 (a) M. P. Kang, D. B. Luo, X. C. Luo, Z. Y. Chen and Z. E. Lin, *CrystEngComm*, 2012, **14**, 95; (b) H. L. Sun, X. L. Wang, L. Jia, W. Cao, K. Z. Wang and M. Du, *CrystEngComm*, 2012, **14**, 512; (c) S. L. Xiang, J. Huang, L. Li, J. Y. Zhang, L. Jiang, X. J. Kuang and C. Y. Su, *Inorg. Chem.*, 2011, **50**, 1743; (d) D. B. Cordes and L. R. Hanton, *Inorg. Chem.*, 2007, **46**, 1634; (e) X. T. Zhang, L. M. Fan, X. Zhao, D. Sun, D. C. Li and J. M. Dou, *CrystEngComm*, 2012, **14**, 2053; (f) M. Chen, S. S. Chen, T. Okamura, Z. Su, M. S. Chen, Y. Zhao, W. Y. Sun and N. Ueyama, *Cryst. Growth Des.*, 2011, **11**, 1901; (g) X. M. Jing, H. Meng, G. H. Li, Y. Yu, Q. S. Huo, M. Eddaoudi and Y. L. Liu, *Cryst. Growth Des.*, 2010, **10**, 3489.
- 75 (a) Y.-Q. Chen, S.-J. Liu, Y.-W. Li, G.-R. Li, K.-H. He, Y.-K. Qu, T.-L. Hu and X.-H. Bu, *Cryst. Growth Des.*, 2012, **12**, 5426; (b) H. Yao, L. Long-Jiang, Z. Ming-Shan, Z. Xiao-Jun, Z. Chao, F. Fei-e and Z. Yong-Ming, *Z. Anorg. Allg. Chem.*, 2013, **639**, 1884.
- 76 (a) B. R. Manzano, F. A. Jalon, M. L. Soriano, M. C. Carrion, M. P. Carranza, K. Mereiter, A. M. Rodriguez, A. de la Hoz and A. Sanchez-Migallon, *Inorg. Chem.*, 2008, **47**, 8957; (b) C. L. Chen, C. Y. Su, Y. P. Cai, H. X. Zhang, A. W. Xu, B. S. Kang and H. C. zur Loya, *Inorg. Chem.*, 2003, **42**, 3738; (c) M. J. Hannon, C. L. Painting, E. A. Plummer, L. J. Childs and N. W. Alcock, *Chem. – Eur. J.*, 2002, **8**, 2225; (d) J. R. Price, Y. Lan, G. B. Jameson and S. Brooker, *Dalton Trans.*, 2006, 1491.
- 77 Q. Shi, L. J. Xu, J. X. Ji, Y. M. Li, R. H. Wang, Z. Y. Zhou, R. Cao, M. C. Hong and A. S. C. Chan, *Inorg. Chem. Commun.*, 2004, **7**, 1254.
- 78 (a) C. S. Campos-Fernandez, B. L. Schottel, H. T. Chifotides, J. K. Bera, J. Bacsa, J. M. Koomen, D. H. Russell and K. R. Dunbar, *J. Am. Chem. Soc.*, 2005, **127**, 12909; (b) B. L. Schottel, H. T. Chifotides, M. Shatruk, A. Chouai, L. M. Perez, J. Bacsa and K. R. Dunbar, *J. Am. Chem. Soc.*, 2006, **128**, 5895.
- 79 (a) B. Moulton and M. J. Zaworotko, *Chem. Rev.*, 2001, **101**, 1629; (b) M. R. Kishan, J. Tian, P. K. Thallapally, C. A. Fernandez, S. J. Dalgarno, J. E. Warren, B. P. McGrail and J. L. Atwood, *Chem. Commun.*, 2010, **46**, 538; (c) K. J. Hartlieb, A. K. Blackburn, S. T. Schneebeli, R. S. Forgan, A. A. Sarjeant, C. L. Stern, D. Cao and J. F. Stoddart, *Chem. Sci.*, 2014, **5**, 90; (d) X. C. Huang, J. P. Zhang and X. M. Chen, *J. Am. Chem. Soc.*, 2004, **126**, 13218; (e) G. Mezei, P. Baran and R. G. Raptis, *Angew. Chem., Int. Ed.*, 2004, **43**, 574; (f) J. P. Zhang, X. C. Huang and X. M. Chen, *Chem. Soc. Rev.*, 2009, **38**, 2385; (g) S.-S. Chen, M. Chen, S. Takamizawa, P. Wang, G.-C. Lv and W.-Y. Sun, *Chem. Commun.*, 2011, **47**, 4902; (h) Z. M. Hao and X. M. Zhang, *Cryst. Growth Des.*, 2007, **7**, 64; (i) I. Boldog, J. Sieler and K. V. Domasevitch, *Inorg. Chem. Commun.*, 2003, **6**, 769; (j) B. Zimmer, V. Bulach, M. W. Hosseini, A. De Cian and N. Kyritsakas, *Eur. J. Inorg. Chem.*, 2002, 3079.
- 80 M. Du, C.-P. Li, C.-S. Liu and S.-M. Fang, *Coord. Chem. Rev.*, 2013, **257**, 1282.
- 81 S.-N. Wang, J. Bai, Y.-Z. Li, Y. Pan, M. Scheerb and X.-Z. You, *CrystEngComm*, 2007, **9**, 1084.
- 82 (a) C. Janiak, *Dalton Trans.*, 2003, 2781; (b) Y. Cui, Y. Yue, G. Qian and B. Chen, *Chem. Rev.*, 2011, **112**, 1126; (c) Z. Hu, B. J. Deibert and J. Li, *Chem. Soc. Rev.*, 2014, **43**, 5815.
- 83 (a) M. D. Allendorf, C. A. Bauer, R. K. Bhakta and R. J. T. Houk, *Chem. Soc. Rev.*, 2009, **38**, 1330; (b) G. Accorsi, A. Listorti, K. Yoosaf and N. Armaroli, *Chem. Soc. Rev.*, 2009, **38**, 1690; (c) R. C. Evans, P. Douglas and C. J. Winscom, *Coord. Chem. Rev.*, 2006, **250**, 2093.
- 84 T. T. Yeh, J. Y. Wu, Y. S. Wen, Y. H. Liu, J. T. Wu, Y. T. Tao and K. L. Lu, *J. Chem. Soc., Dalton Trans.*, 2005, 656.
- 85 Y. B. Dong, Y. Geng, J. P. Ma and R. Q. Huang, *Inorg. Chem.*, 2005, **44**, 1693.
- 86 S. Muthu, Z. Ni and J. J. Vittal, *Inorg. Chim. Acta*, 2005, **358**, 595.

- 87 H. Schmidbaur and A. Schier, *Angew. Chem., Int. Ed.*, 2015, **54**, 746.
- 88 V. W.-W. Yam and K. K.-W. Lo, *Chem. Soc. Rev.*, 1999, **28**, 323.
- 89 W. Chen, J. Y. Wang, C. Chen, Q. Yue, H. M. Yuan, J. S. Chen and S. N. Wang, *Inorg. Chem.*, 2003, **42**, 944.
- 90 (a) T. H. Kim, Y. W. Shin, J. H. Jung, J. S. Kim and J. Kim, *Angew. Chem., Int. Ed.*, 2008, **47**, 685; (b) I. O. Koshevoy, C. L. Lin, A. J. Karttunen, M. Haukka, C. W. Shih, P. T. Chou, S. P. Tunik and T. A. Pakkanen, *Chem. Commun.*, 2011, **47**, 5533; (c) J. H. Liang, Z. Chen, J. Yin, G. A. Yu and S. H. Liu, *Chem. Commun.*, 2013, **49**, 3567; (d) X. C. Shan, F. L. Jiang, D. Q. Yuan, H. B. Zhang, M. Y. Wu, L. Chen, J. Wei, S. Q. Zhang, J. Pan and M. C. Hong, *Chem. Sci.*, 2013, **4**, 1484; (e) S. Perruchas, X. F. Le Goff, S. Maron, I. Maurin, F. Guillen, A. Garcia, T. Gacoin and J. P. Boilot, *J. Am. Chem. Soc.*, 2010, **132**, 10967; (f) D. Sun, S. Yuan, H. Wang, H.-F. Lu, S.-Y. Feng and D.-F. Sun, *Chem. Commun.*, 2013, **49**, 6152.
- 91 (a) B. Li, R. W. Huang, J. H. Qin, S. Q. Zang, G. G. Gao, H. W. Hou and T. C. W. Mak, *Chem. – Eur. J.*, 2014, **20**, 12416; (b) D. Sun, L. L. Zhang, H. F. Lu, S. Y. Feng and D. F. Sun, *Dalton Trans.*, 2013, **42**, 3528.